

A STUDY OF THE TRANSMUTATION  
OF NITROGEN BY PROTONS

Thesis by  
Donal Baker Duncan

In Partial Fulfillment of the Requirements  
For the Degree of  
Doctor of Philosophy

California Institute of Technology  
Pasadena, California

1951

## ABSTRACT

An experimental investigation has been made of the cross section for the  $N^{14}(p\gamma)O^{15}$  reaction using protons accelerated by an electrostatic generator. Excitation curves have been obtained from  $Be_3N_2$  targets, nitrogen gas targets, and a thin target formed by proton bombardment of a copper foil in a nitrogen atmosphere. It has been found possible to describe the experimental cross section from .250 to 2.6 Mev by assuming the existence of nine resonances. The parameters appropriate for a theoretical description of the resonances are determined from the experimental data. The yields from the various resonances are extrapolated to the low energies corresponding to stellar temperatures. It has not been possible to make more than very uncertain assignment of such properties as the angular momentum and parity for the excited levels in  $O^{15}$  that are indicated by the cross section.

## ACKNOWLEDGMENTS

Research in experimental nuclear physics today is a highly cooperative venture. This thesis could never have been written without the aid of many people. I wish to express my indebtedness to Professor C. C. Lauritsen for the opportunity of working in Kellogg Laboratory, and to thank him and Professor William A. Fowler for having suggested the subject of this investigation.

I wish to acknowledge most gratefully the active cooperation of Dr. Joseph Perry in designing the experimental apparatus, taking the data and organizing it. Many discussions with Dr. Fowler, Dr. Perry and Professor Robert F. Christy were very helpful. Among the others who contributed their time are Mr. Robert Day in taking data, Mr. Victor Ehrgott in designing mechanical apparatus, Mr. Lloyd Gilliland and Mr. George Fastle in doing the machine work, and Mr. William Gibbs in building and repairing electronic components of the apparatus.

I held a fellowship from the Atomic Energy Commission during most of the time that this research was carried out and a teaching fellowship from the California Institute of Technology for several preceding years. The research was jointly sponsored by the Office of Naval Research and the Atomic Energy Commission.

I wish to thank all of these and the other members of the faculty of the California Institute of Technology, and the staff of the Kellogg Radiation Laboratory, for having contributed their time and made possible this investigation.

## TABLE OF CONTENTS

<u>Part</u>	<u>Title</u>	<u>Page</u>
I	Introduction . . . . .	1
II	Experimental Procedure and Apparatus . . . . .	1
III	Experimental Results . . . . .	13
IV	Discussion of Experimental Results . . . . .	16
	References . . . . .	37
	Figures . . . . .	38

## I- INTRODUCTION

The accumulation of experimental data on the properties of energy levels in the various light nuclei represents one of the major fields of nuclear research. The primary purpose of this investigation was to determine the properties of the levels in  $O^{15}$  attained by bombarding  $N^{14}$  with protons. The particular reaction studied is also of direct interest as being one of the postulated sources of stellar energy.

When protons bombard  $N^{14}$  there is a certain probability that they will be captured to form  $O^{15}$  in an excited state. This compound nucleus will decay in all the modes that are energetically possible; for example by the emission of a gamma ray, a proton, a neutron, or an alpha particle. In general the probability of producing each of these reactions can be studied as a function of proton energy. However, the threshold for the  $N^{14}(p \alpha)C^{11}$  reaction is 3.2 Mev and for the  $N^{14}(p n)O^{14}$  reaction is 6 Mev, so that at the available proton energies, the only transmutation possible was by  $N^{14}(p \gamma)O^{15}$

Very little experimental knowledge had been previously obtained on this reaction. Early workers with cyclotrons had observed that 2 minute activity was produced by bombarding nitrogen with protons (1) but had accumulated little knowledge of the energy dependence of the activation. Using a Cockroft-Walton machine, Curran and Struthers (2) had investigated the region from 450 to 950 kev. They found an exceptionally low yield and little evidence for any resonant structure. Tangen (3) studied the region from 260 kev to 550 kev, finding a resonance at 277 kev. In their study of the sun-cycle reactions; Woodbury, Hall, and Fowler (4) bombarded nitrogen

with protons of 128 kev energy. The completion of an electrostatic generator capable of reaching energies somewhat above 2.5 Mev permitted the investigation of the large unexplored energy range as well as the problem of checking previous work.

Since it was expected that the yield would be quite low, it was decided to detect the reaction by means of the positrons emitted by  $O^{15}$  as it decays to  $N^{15}$ , since they can be counted with a much higher efficiency than the immediate  $\gamma$ -ray. This process has other definite advantages. No corrections are necessary for the  $\gamma$ -rays produced when protons bombard  $N^{15}$  or any other element present. If any radioactivity was produced by another reaction, that fact became apparent by the departure of the decay from a 2 minute half life and the cause of the additional counts could be investigated. The counting process could be carried out without high voltage on the electrostatic generator with a corresponding decrease in the background counting rate.

It was felt that the choice of the proper target material would be a particularly critical one. Two possible errors can be introduced. There may be an appreciable escape of the radioactive oxygen from the target into the vacuum system; the target compound may decompose chemically. This latter problem is present in any work of this kind, but it might be particularly serious in this case because of the relatively unstable nature of most nitrogen compounds. By using a gas target chamber containing chemically pure nitrogen, both of these sources of error are removed. Unfortunately, other complications are introduced; the most important of which is a large spread in the energy of the proton beam after it has passed through an entrance foil. Solid targets were therefore necessary to investigate the details of any sharp resonant

structure. Beryllium nitride and a thin nitrogen layer absorbed on a copper foil were used. Yields from these targets were calibrated by yields from gas targets.

## II-EXPERIMENTAL PROCEDURE AND APPARATUS

The protons were accelerated by an electrostatic generator of the type described in many places in the literature.<sup>(5)</sup> They were analyzed by a double focusing magnetic analyzer.<sup>(6)</sup> The strength of the field was determined by means of a null-reading magnetometer of the type constructed and used in this laboratory by Professors C. C. Lauritsen and T. Lauritsen.<sup>(7)</sup> The type of magnetometer they described was slightly modified, the null-point being detected by having a light patch reflected from a mirror on the coil fall on a split photo-tube.

No attempt was made to determine the proton energy absolutely, the resonances in the  $\text{Al}(p, \gamma)$  and  $\text{F}(p, \alpha \gamma)$  reactions at .9933 Mev and .8735 Mev being used as calibration standards.<sup>(8)</sup> The proton energy is given by  $E = k(mv)^{-2}$  where  $E$  is the proton energy in Mev,  $k$  is the magnetometer constant, and  $mv$  is the voltage drop in millivolts produced by the magnetometer balance current as read on a potentiometer.

The aluminum reaction proved to be the most useful for calibration. Excitation curves were obtained immediately before and after any nitrogen bombardments where the magnetometer constant was needed accurately. A freshly turned aluminum rod, slightly rotated after each bombardment to prevent the accumulation of carbon layers was used as a target. Thick target excitation curves showed a half width of 1 kev; this giving the value of the energy resolution, since the width of the reaction is known to be less than 300 ev.<sup>(8)</sup> A typical curve is given in Figure 1. For a time considerable drift was observed, the magnetometer constant  $k$



changing by as much as .5% during a day. A procedure of re-checking the zero every 6 minutes during a bombardment was adopted and results consistent to better than .1% were obtained at all later times.

All the values of k used in converting the nitrogen bombardment curves to an energy scale were obtained from bombarding aluminum with protons. Excitation curves were also obtained for the  $F(p, \alpha \gamma)$  reaction and for the same aluminum resonance bombardment with ionized hydrogen molecules. <sup>(HHT)</sup> No detectable dependence of the magnetometer constant on energy was indicated by these reactions.

In addition to the energy of the proton, it is necessary to know the transmutations per incident proton produced by a particular target. A formula connecting this yield with measurable quantities can be derived as follows: Let

- y = number of transmutations produced per proton.
- n = number of protons per second incident on the target
- $\lambda$  = decay constant of  $O^{15}$
- $t_1$  = length of time that the target is bombarded
- $t_2$  = length of time counts are recorded
- $c_0$  = number of counts recorded
- c = number of counts corrected for previous bombardment  
and for background counts
- f = efficiency of particular experimental setup for  
detecting positrons

The number of  $O^{15}$  atoms formed at time  $\tau$  during element of time  $d\tau$  during bombardment is  $nyd\tau$ . The number of these present at a later time t is  $nye^{-\lambda(t-\tau)} d\tau$ . Differentiating this with respect to time gives the number of positrons produced at time t in

a time interval  $dt$  as  $n\lambda ye^{-\lambda(t-\tau)}d\tau dt$ . Integrating this from  $\tau = 0$  to  $\tau = t_1$  and from  $t = t_1$  to  $t = t_2 + t_1$  gives as an expression for the total number of positrons produced in a length of time  $t_2$  immediately after having bombarded for a time  $t_1$ ,

$$\left[ \frac{ny}{\lambda} (1 - e^{-\lambda t_1})(1 - e^{-\lambda t_2}) \right] \quad (1)$$

It is necessary to correct this for the activity produced during the previous bombardment. If there were  $c_0$  counts during a counting period equal to  $t_2$  and there has been a period  $t_3$  between the end of the counting period and bombarding again, the correction term will be

$$\left[ c_0' = c_0 e^{-\lambda(t_1 + t_2 + t_3)} \right] \quad (2)$$

One thus obtains for the number of counts due to the bombardment in question  $c = c_0 - c_0' - b$ . If  $f$  is the efficiency of counting these positrons, a final expression for the yield  $y$  in transmutations per proton is

$$y = \frac{c\lambda}{nf(1 - e^{-\lambda t_1})(1 - e^{-\lambda t_2})} \quad (3)$$

The quantities to be measured are therefore  $c$ ,  $t_1$ ,  $t_2$ ,  $n$ ,  $\lambda$ , and  $f$ .

The total number of counts was obtained from a Geiger-Müller counter located in a fixed geometrical position. For absolute work with gas targets a thin window bell-jar counter was used; for most of the excitation curves a thin wall cylindrical type counter was used, since its plateau curve seemed to drift less over long periods of time. The drifts were checked by obtaining

the counting rate from a thorium source and the yields at specified energies periodically.

The lengths of time of bombardment and counting were controlled automatically by a synchronous motor driving a stepping relay. The times that were normally chosen were two minutes of bombardment, three minutes of counting with the electrostatic generator voltage off, and one minute before bombarding again.

The number of protons hitting the target was determined by an integrator constructed by Dr. A. B. Brown. The charge went onto a condenser whose capacitance is  $C$  measured in microfarads, the integrator being calibrated to fire at a definite voltage,  $V_0$ . The number of times the integrator discharged,  $N$  was counted on a mechanical counter, and the voltage on the condenser at the end of a bombardment,  $V$ , was read directly off a meter on the integrator which had been previously calibrated. If it is assumed that the beam strength is constant, the number of protons per second,  $n$ , is equal to  $(6.242 \times 10^{12}) \frac{(NV_0 + V)}{t}$ ,  $V_0$  and  $V$  were calibrated from a .1% meter. The capacitance,  $C$ , was measured both by an a.c. bridge and by a d.c. deflection method. The latter was done by Mr. John Reeds. Consistent values were obtained whose average was 0.287 microfarads.

The half life of  $O^{15}$ , which is related to  $\lambda$  by  $\lambda T_{\frac{1}{2}} = \log_e 2$ , has been previously measured. A tabulation of values is given below:

TABLE 1

Half life	Observer
126 $\pm$ 5	McMillan and Livingston, Phys. Rev. <u>47</u> , 452 (1935)
130 $\pm$ 6	Huber, Lienhard, and Sherrer, Helv. Phys. Acta. <u>17</u> , 139 (1944)
126 $\pm$ 3	Sherr, Muether, and White, Phys. Rev. <u>75</u> , 282 (1949)
118 $\pm$ 0.7	Perez-Mendez and Brown, Phys. Rev. <u>76</u> , 689 (1949)

A measurement of T was also made during this work. A least squares fit to the data of Figure 2 gives  $T_{\frac{1}{2}} = 127$  seconds. In calculations  $T_{\frac{1}{2}} = 126$  seconds was used.

The counting efficiency f is the most difficult quantity to measure, and was determined directly only for the gas target. The target chamber for gas targets is pictured in Figure 3, where it is drawn in quarter section view. The proton beam was limited by the aperture stop which was 3/16 inches in diameter, the entrance foil being placed over a hole  $\frac{1}{4}$  inch in diameter. A quartz viewing disc was placed over the end during the preliminary lining-up process and the apparatus adjusted so that the beam went through the center of the foil. This was also checked after bombardment by observing the carbon layer on the foil.

Aluminum was chosen for the entrance foil because it was readily available in foil form and because no radioactive isotopes had been observed from proton bombardment at energies below the threshold for the pn reaction at 5 Mev. At no time was any activity observed which was ascribed to the aluminum. The thinnest foil which seemed to offer any hope of being vacuum tight was 0.00015 inches thick, being made available by the Los Alamos National Scientific Laboratory. It was found possible to make seals with this material which would stand a pressure differential of half an atmosphere across the entrance hole. In cases where a greater pressure differential was desirable, thicker foils were used.

The aluminum foil was "sandwiched" between two brass discs as indicated in the drawing, the seal being made with O-rings. This was found to be a particularly convenient technique, since it

required little manipulation of the foil.

Copper foil 0.001 inches thick was used between the counter and the target. This was thin enough to make the absorption of positrons a comparatively small effect, and yet thick enough to be handled easily and to stop the proton beam at all but the highest energies available with this accelerator. A vacuum tight solder seal was made between this foil and a thin brass ring which fitted over the end of the target assembly.

Standard one-eighth inch needle valves were modified and used as valves. The base was turned down to fit into a slot in the target assembly, the valve seat being made flush with the inside bore. The gas was thus confined to a volume which very closely approximated one of cylindrical symmetry.

The target assembly and counter were surrounded by lead bricks to reduce the background counting rate. The counter was attached to a lead brick and held at a fixed distance from the target.

With this arrangement it should be possible to determine the counting efficiency and an effort was made to do so. It was found necessary to consider the variation of counting efficiency over the face of the counter, the geometrical solid angle subtended by the counter, and the absorption of the positrons in the copper foil.

The variation of counter efficiency over the face of the bell jar counter was determined empirically by using collimated natural beta rays from Radium E. The relative efficiency as determined as a function of  $r$ ,  $\Theta$ , and  $\phi$  is given in Figure 4. The distance

from the center of the counter to the point where the particles enter is defined as  $r$ ;  $\Theta$  and  $\Phi$  are the usual polar angles describing their direction,  $\Phi = 0$  and  $\Theta = 90^\circ$  corresponding to the line from the center to the point in question. These angles are illustrated in Figure 5.

If we neglect the absorption of positrons, the counting efficiency from a cylindrical volume can now be formulated analytically. The geometrical picture is given in Figure 5. A point in the gas cylinder can be described by cylindrical coordinates  $\rho$ ,  $\phi'$ , and  $z$ ; the point on the surface of the counter by  $r$  and  $\phi$ . From symmetry the result is independent of  $\phi'$  which may be taken as 0. The efficiency is then given by

$$\frac{\int_0^{z_0} \int_0^{\rho_0} \int_0^\pi \int_0^r \frac{\cos \Theta}{R^2} \epsilon(r, \Theta, \Phi) \rho r d\phi d\phi' dz}{2 \int_0^{z_0} \int_0^{\rho_0} \int_0^\pi \int_0^\infty \frac{\cos \Theta}{R^2} \rho r d\phi d\phi' dz} \quad (4)$$

where  $\epsilon(r, \Theta, \Phi)$  is the measured counting efficiency, assumed to be 100% for  $r = 0$ ,  $\Theta = 0^\circ$ , and

$$\begin{aligned} R^2 &= (\rho - r \cos \phi)^2 + (z_1 - z)^2 + r^2 \sin^2 \phi \\ \cos \Theta &= (z_1 - z)R^{-1} \\ \sin \Phi &= \rho \sin \phi \left\{ (\rho - r \cos \phi)^2 + r^2 \sin^2 \phi \right\}^{-\frac{1}{2}} \end{aligned} \quad (5)$$

The integral in the denominator can be evaluated by inspection;  $r$  and  $\phi$  integrations give one-half of the surface of a sphere,  $\rho$  and  $z$  integrations give the volume of the "pie-shaped" sector.

It was necessary to evaluate the integral in the numerator numerically. This has been done using Simpson's Rule, each of the variables of integration being given three values.

To correspond to the experimental apparatus, it is also necessary to consider the small volume behind the main cylinder. The counting efficiency for this volume may be expressed by similar integrals. Because of the small volume of gas involved, the numerical integration was done by taking mean values.

For the particular setup used:  $r_0 = 9$ ,  $\rho_0 = 8$ ,  $Z_0 = 17.472$ , and  $Z_1 = 26.04$ , where the distances are expressed in sixteenths of an inch. The counter was moved back from the target considerably more than was mechanically necessary; it was hoped that this would increase the accuracy with which the integrals could be evaluated.

With these values a counting efficiency of the main volume of 3.71% and of the smaller volume of 0.81% was obtained. Averaging these according to their corresponding volumes gives an over-all efficiency of 3.70%.

The correction for absorption of the positrons in the copper foil was determined empirically. The yield from a thick air target bombarded at 1.6 Mev was obtained as a function of absorber thickness. An extrapolation was then made to zero thickness. The thin window bell jar counter was used to detect the radiation. A thick target was desirable because of larger counting rates with increased statistical accuracy. An air target of atmospheric pressure was used because it minimized the errors arising from pressure variations and because it permitted the use of very thin and therefore

not completely vacuum tight absorbers between the target and the counter. It had been previously determined that oxygen gave negligible activity at this energy of bombardment, although considerable 70 second activity was observed from the bombardment of such a target at 2.5 Mev. The results of this experiment are given in Figure 6. The data indicates a linear decrease of yield with  $\text{mg}/\text{cm}^2$  of absorber. Assuming this, a least squares fit was made to the data, giving a correction of 13% to be applied when data is obtained with one mil copper foil between the target and the counter. Using these values a final value of  $f = 3.30\%$  was obtained for the bell jar counter.

To calibrate the data of the excitation curves obtained with the cylindrical counter it is only necessary to determine the yield from this air target with the same counter and geometry used during bombardment and compare this with the yield using the bell jar counter. Doing this gives a counting efficiency of 4.41% for the cylindrical counter.

With the gas target it is not only possible to determine relative and absolute yields from a particular thickness of target, but having determined the thickness in atoms per square centimeter it is possible to make a direct measurement of the cross section under certain conditions. The yield from a nuclear reaction produced by protons of energy  $E$  is given by  $y(E) = \int_0^t \sigma(x)n dx$ , where  $\sigma$  is the cross section,  $n$  is the numerical density of disintegrable atoms,  $x$  is the distance the proton has penetrated the target, and  $t$  is the thickness. If this expression is integrated over the energy distribution of the protons, a final equation is determined



for the yield. In the special case, which was often satisfied in this experiment, that the variations of  $\sigma$  over the energy ranges corresponding to the target thickness and the spread of energy in the proton beam, this reduces to  $y = \sigma nt$ .

The cross section can therefore be determined from a measurement of  $t$  and  $n$ . A convenient expression for  $n$  is given by  $n = 2n_0 \left( \frac{p}{p_0} \right) \left( \frac{T_0}{T} \right)$ , where  $n_0$  is the Lodschmidt number evaluated at a standard pressure and temperature ( $p_0$  and  $T_0$ ), and  $p$  and  $T$  are the observed pressure and temperature. Throughout all the experiments the temperature remained essentially constant at  $24^\circ\text{C}$ . The pressure was measured with an oil manometer filled with octoil, whose density at this temperature was measured to be  $0.979 \text{ mg/cm}^3$ . The target chamber was first evacuated with oil diffusion pumps, flushed several times with nitrogen, filled to a specified pressure as read on the manometer, and then sealed off with the needle valve. The distance  $t$  was determined with sufficient accuracy with a micrometer and a depth gauge to be 3.11 cm. The pressure was usually about 22.0 cm. of octoil, in which case  $nt$  can be evaluated to be  $3.21 \times 10^{18} \text{ atoms/cm}^2$ .

It was found that the yield from a given gas target would decrease with time, indicating that some of the nitrogen was leaking into the vacuum system. This effect was never completely eliminated. A given target was therefore bombarded for only a short time; yields at a specified voltage were taken several times during the run and a linear correction was applied to other points. This correction amounted to about 1.5% per hour and was usually unimportant compared with counting statistics.

After bombarding for several days, two minute activity was observed from bombarding the target chamber before it was filled with nitrogen. This activity was observed to come from the spot where the proton beam had been hitting the copper foil. To obtain cross section values it was therefore necessary to obtain plots of the yield against pressure. These are shown in Figure 7 and are seen to be linear and to have a non-zero intercept. A least squares fit to this data was used to obtain the best value of the cross section at these particular energies. From them an estimate can be obtained to apply to other data to correct for this "vacuum activity". This correction for a target of 23 cm. of oil pressure was found to be 17%.

The thin layer of nitrogen which had been absorbed on the copper foil thus necessitated an appreciable correction to the gas target data. It did however furnish a convenient thin target which was used to investigate the details of the resonant structure. A target 7 kev thick at 1 Mev and approximately 10% nitrogen was formed after microampere-hours of proton bombardment. This would seem to furnish a useful technique for forming thin targets where the target material is available in gaseous form.

For thick target work, pressed  $\text{Be}_3\text{N}_2$  targets were used. The chemical stability of nitrides in comparison to most nitrogen compounds indicated they would be most useful as targets. TiN was used but found to give a 33 minute activity at high proton energies. Beryllium was chosen because it was known to give no activity upon proton bombardment and the compound was readily available in powder form. A standard target chamber was used

with a one mil copper foil over the side to permit the positrons to reach the nearby counter.

The counting efficiency for this setup can be measured as was done for the gas target. Such a determination will still not guarantee that correct values of the absolute yield are being obtained because of the possibility of the loss of the radioactive oxygen from the target. It was felt that the determination of the counting efficiency of the gas target setup was most reliable, and data from the solid targets was normalized to fit those results in a way that will be described later.

### III-EXPERIMENTAL RESULTS

The results of this experiment are most conveniently expressed by graphs of yield against proton bombarding energy. These will be given for the various types of targets used.

The excitation curve for the bombardment of  $\text{Be}_3\text{N}_2$  is given in Figure 8. The data was obtained as relative yield against proton energy. The ordinate was normalized to give yield in transmutations per incident proton with data from thin gas targets as will be described below. The curve indicates the general nature of the cross section for the reaction; several resonances superimposed on a steadily rising background.

Fresh targets were prepared often, particularly while taking data near the resonances to minimize the shift in energy scale from carbon layers on the target. The yield was monitored at definite energies throughout all the runs to check on decomposition of the target. Apparently the target did not lose nitrogen during the few hours a particular target was bombarded.

The data from bombarding thin gas targets, approximately 20 kev of proton energy thick, is presented in Figure 9. It has been corrected for absorption of the positrons, for activity produced by nitrogen absorbed on the copper foil, and for leakage of nitrogen from the target chamber into the vacuum system. Yield has been plotted against the mean energy of the proton beam after passing through the aluminum foil. This was determined by plotting the measured magnetometer millivolts at the resonances against proton energy for these resonances as determined from the  $\text{Be}_3\text{N}_2$  excitation curve and extrapolating between these points with the known variation of the range of protons in aluminum. (9)

As indicated in the previous discussion, the cross section is directly proportional to the yield from such a target wherever the variation of the cross section is small over the energy range corresponding to the thickness of the target and the spread in energy of the proton beam. This is seen to be valid everywhere except near the resonances and, except near them, the ordinate can be normalized to read directly in square centimeters. It is also approximately true near the small resonance at 1.55 Mev, where the observed width is about twice that of the others. The observed widths of the other resonances, about 40 kev, even with very thin targets, are much larger than the corresponding widths on solid target curves, indicating that the spread in energy of the beam is large in comparison to the true width. This is ascribable to the straggling of the protons in the aluminum and variations in thickness of the foil over the diameter of the beam.

The half life of the activity at each of the resonances and at several of the intermediate points was checked to be the correct value. Particular care was used near the 1.55 Mev resonance to guarantee that it was not due to carbon contamination, since the energy of the protons before passing through the aluminum foil corresponded approximately with the known resonance in the  $C^{12}(p\gamma)$  reaction at 1.7 Mev. However there was no measurable 10 minute activity present.

At the lower energies a thick target excitation curve was obtained using a one atmosphere nitrogen gas target and is given

in Figure 10. It was necessary to use thicker aluminum foil both to support the pressure of the gas and to decrease the proton energy to the lower energies. Yield calibrated by comparison with the  $\text{Be}_3\text{N}_2$  target, is plotted against mean proton energy determined as before by calibrating on the resonance energies and extrapolating between them with the proton range curve. In this case Tangen's value of 277 kev for the very low energy resonance was used.

Professor W. A. Fowler also kindly made available data obtained from a  $\text{NaNO}_2$  target bombarded at energies between 300 and 1300 kev by the other electrostatic generator in the Kellogg Laboratory. This data, which was particularly useful in the region from 600 to 1000 kev, as well as that obtained with the thick gas target and  $\text{Be}_3\text{N}_2$  targets is also given in Figure 10.

Excitation curves were also obtained over various energy ranges with gas targets of intermediate thicknesses, one of which is given in Figure 11. This curve serves to confirm the general nature of the cross section in this region and to give additional values for the thick target step at the resonances.

The thin layer of nitrogen absorbed on the copper foil was also used as a target; the gas target assembly was employed with the aluminum foil removed to eliminate the spread in energy of the proton beam. No decrease in yield corresponding to loss of nitrogen from the target was observed. However discrepancies in comparing the yield from this target and from the gas target at various energies were obtained which could be attributed to the non-uniform nature of the nitrogen layer and small movements of the proton beam with energy. Copious quantities of 10 minute

activity at low energies and near 1.7 Mev were obtained which are ascribable to carbon on the target. This yield was large enough to make it impossible to obtain excitation curves of the 1.55 and 1.748 Mev resonances and it was necessary to determine their structure from other excitation curves. The excitation curves for various resonances are given in Figures 12, 13, and 14. Because of the very low yield from this target, statistical errors are larger than in any other curves. Nevertheless they proved to be quite useful in determining the details of resonant structure.

#### IV-DISCUSSION OF EXPERIMENTAL RESULTS

It has been found convenient to describe the properties of the energy levels in the light nuclei in terms of certain parameters. The following are often employed: proton energy to produce resonance,  $E_R$ ; thick target step,  $Y_{\max}(\infty)$ ; cross section at resonance,  $\tilde{\sigma}_R$ ; observed resonance width,  $\Gamma'$ ; target width,  $\xi$ ; true nuclear width,  $\Gamma$ ; partial nuclear width,  $\omega\gamma$ ; proton width,  $\Gamma_p$ ; and proton width at 1 Mev without Coulomb barrier,  $G$ . In their paper on gamma radiation Fowler, Lauritsen, and Lauritsen<sup>(10)</sup> give precise definitions of these quantities and in addition show that if the cross section follows the Breit-Wigner dispersion formula there are certain relationships between them. Neglecting the variations of  $\lambda$  and  $\Gamma_p$  with energy over the energy range of the resonance, they obtain the following equations:

$$Y_{\max}(\infty) = \frac{\pi}{2} \frac{\tilde{\sigma}_R \Gamma}{\xi} \quad (6)$$

$$\Gamma' = (\Gamma^2 + \xi^2)^{\frac{1}{2}} \quad (7)$$

$$\omega\gamma = \frac{2 \xi Y}{\lambda^2} \quad (8)$$

They also quote a general result derived by Bernet et. al, that, independent of the homogeneity of the bombarding protons or the exact nature of the thin target excitation curve, the integrated area under the curve,  $A(\xi)$  is given by

$$\xi Y_{\max}(\infty) = A(\xi). \quad (9)$$

Using these equations the various parameters for the indicated resonances can be estimated from the experimental data. A final tabulation of the properties is given later in Table 2.

The resonance energy,  $E_R$ , is determined most accurately from the thick target  $\text{Be}_3\text{N}_2$  excitation curve. Using the data of the gas target would be inaccurate because the energy loss of the protons in the aluminum is uncertain; the thin target curves are shifted a small amount by the layers of carbon on the surface. Estimates were made of the thick target step at each of the resonances. It is then easily shown that the proton energy necessary to give one half of this step is the resonance energy. In this way values of  $E_R$  equal to 1.065, 1.748, 1.815, 2.356, and 2.489 Mev were determined.

Two additional resonances are indicated immediately in the data which cannot be handled this way. The very low energy resonance indicated on Figure 10 could not be studied with the solid target because the electrostatic generator would not operate successfully at this low an energy. Tangen's<sup>(3)</sup> value of 277 kev for  $E_R$  at this resonance has been accepted. There is also the small resonance at about 1.5 Mev shown on the gas target curves in Figures 9 and 11, but too weak to be observed with the other targets. The technique used to determine the resonance energy here was to



employ the proton energy scale for the gas target curve obtained as described above. In this way a value of 1.55 Mev was obtained.

Relative values for the thick target steps at the first described resonances are immediately available from the  $\text{Be}_3\text{N}_2$  curve, having been obtained in the process of determining  $E_R$ . To obtain absolute values it is necessary to determine the geometry of the solid target assembly or to measure one of the steps in another way.

The data from the gas target provides a convenient method of obtaining  $Y_{\text{max}}(\infty)$  at the 1.065 resonance. From Equation 9, the thickness of the target and the area under the curve determine the desired quantity. The target thickness in atoms per square centimeter has already been found. Multiplying this by the stopping cross section for nitrogen at this energy gives  $\xi$ . The area under the curve was obtained by integrating numerically using Simpson's rule, a process quite accurate in this case since a large number of points were available. Since the counting efficiency of the gas target setup has been evaluated above, this gives immediately a value for  $Y_{\text{max}}(\infty)$  at this resonance, which was  $5.5 \times 10^{-10}$  transmutations per proton incident on a  $\text{N}_2$  target.

This process can also be applied to the resonances at higher energies. However it becomes less accurate because of the uncertainty as to what part of the yield to ascribe to the "non-resonant" background. This becomes particularly true at around 2.5 Mev. For this reason, the thick target data was used.

To compare the curves, it is necessary to have the stopping cross section for nitrogen gas and for the nitrogen in beryllium nitride. The first is 0.986 that of air which is given by Bethe. (12)

For the latter the stopping cross section of beryllium is needed. This has been measured from 500 kev to 1400 kev by Madson and Venkateswarlu.<sup>(13)</sup> They have determined the parameters in the appropriate theoretical formula to fit the data in this region. The theory of stopping cross sections is sufficiently well understood to indicate that their formula will give the correct values when extrapolated to the higher energies required.

In this way the thick target yield from a  $\text{Be}_3\text{N}_2$  target at the resonance is computed to be  $2.8 \times 10^{-10}$  transmutations per proton. This figure can then be used to normalize the entire  $\text{Be}_3\text{N}_2$  excitation curve. The thick target steps at the other resonances observed on it can be read off directly. In Table 2, this information has been retabulated as the yield from a  $\text{N}_2$  target to give some kind of uniformity to the values obtained from different targets.

Having determined the value for the thick target step at one of the resonances, all of the thick target data which was taken only in a relative way can be normalized. Thus the ordinate was obtained for the data from the thick gas target, the semi-thick gas target, and the  $\text{Be}_3\text{N}_2$  target. In addition the data of Professor Fowler was normalized to give this value.

The value of  $Y_{\text{max}}(\infty)$  for the 1.55 Mev resonance can be obtained from the thin gas target in the same way as was done for the 1.065 Mev resonance or from the semi-thick gas target. These values were quite consistent and their average is given. The value at the .277 Mev resonance can be obtained only from the thick gas target.

The values of the nuclear widths can be obtained only from the thick  $\text{Be}_3\text{N}_2$  and thin solid nitrogen target curves for most of

the resonances. Since the width of the 1.55 Mev resonance is about twice the indicated widths of the other resonances on the thin gas target curve, a value for the width can be obtained from this curve. In all other cases the energy resolution determines the widths from this target.

The width of the 1.065 resonance can be determined quite satisfactorily from the thick target curve, and this was done. When this is attempted at the other resonances, the fact that the step is only a relatively small percentage of the total yield makes such an evaluation less accurate. For this reason the thin target curves proved to be more useful.

The observed width from the thin target of the 1.065 Mev resonance was 6.9 kev, compared with the true width as measured from the  $\text{Be}_3\text{N}_2$  target of 4.8 kev. This indicates a target thickness of 5 kev. The variation of the thickness with energy is given by  $\xi = \epsilon nt$ , where the cross section may be taken with sufficient accuracy as proportional to that of air. At higher energies this thickness becomes small in comparison to the observed widths and only a small correction must be made to determine the true width. Making this correction to the observed widths, values of  $\Gamma$  are determined from each of the thin target curves.

For the resonance at 1.748 Mev the only data available was from the thick target curve and that was used. For the .377 Mev resonance no data was obtainable and Tangen's<sup>(3)</sup> result that the width is less than 2 kev is quoted.

Having obtained for these various resonances values of  $Y_{\max}(\infty)$  and  $\Gamma$ ,  $\sigma_R$  is immediately calculable from Equation 6. This calculation has been carried through for the various cases

and tabulated in Table 2.

It is now possible to subtract out the yield from these resonances in both the thin and thick target curves to look for an adequate description of the remaining "non-resonant" yield. The experimental values for the cross section for this yield are given in Figure 15. The data from the gas target curve represents merely a replotting of the data of Figure 9, the points near the resonances being omitted or a smooth curve being drawn through the base of the resonances.

Since  $\sigma = \epsilon \frac{dY}{dE}$ , values for the cross section can also be obtained by differentiating the thick target curve. The data at high energies obtained in this way is less accurate than that from the thin gas target and is given only to indicate the degree of consistency between the two curves. The values at lower energies could only be obtained in this way. The cross section in the region from 400 to 900 kev is best obtained by numerically differentiating the excitation curve of the  $\text{NaNO}_2$  target.

There are two striking features of this cross section. The first is that the over-all picture resembles that of a resonance centered at about 2.5 Mev. An attempt was made to fit the experimental points with a cross section of the Breit-Wigner form

$$\sigma = \pi \lambda^2 \frac{\Gamma_p \Gamma_\gamma}{(E - E_R)^2 + \frac{1}{4} (\Gamma_p + \Gamma_\gamma)^2} \quad (10)$$

where  $\Gamma_p = E^{\frac{1}{2}} P_G$ . The function  $E^{\frac{1}{2}} P$  has been plotted by Christy and Latter<sup>(14)</sup> for the various values of angular momentum which

the proton adds to the compound nucleus. To fit the observed cross section,  $G$  will have to be much larger than any possible values of  $\Gamma_\gamma$ , and the formula can be rewritten in the form

$$\sigma \approx \frac{k}{E} \frac{E^{\frac{1}{2}} P}{(E - E_R)^2 + \frac{1}{4} (E^{\frac{1}{2}} P G)^2} \quad (11)$$

With such a curve,  $E_R$  being chosen equal to 2.5 Mev, it is clearly possible to fit the data at two points, 1.0 and 2.5 Mev. This was done and the resultant curve plotted for s and p wave protons. While the curve for s wave protons had the correct general features, the curve for p wave resembled the data only at low energies and at 2.5 Mev where it had been normalized. For example, the p wave curve gave a cross section four times too large at 1.5 Mev. The situation is presumably worse for protons of higher values of  $l$ .

Having determined that a fit, if any, was to be made with s-wave protons, the process was repeated with various values of  $E_R$ . What appeared to be the best fit was obtained for  $E_R$  equal to 2.6 Mev, although the fit of the curve is not very sensitive to  $E_R$ . With this value a theoretical curve can be drawn which quite adequately represents the experimental points, as can be seen from Figure 15. The "non-resonant" cross section can thus be described in terms of a broad resonance centered at 2.6 Mev. The value of  $\sigma_R$  can be read directly from the curve as  $5 \times 10^{-29} \text{ cm}^2$ . The term  $Y_{\text{max}}(\infty)$  for such a broad resonance does not have much experimental meaning. A value obtained by substituting in Equation 6 values for  $\sigma_R$ ,  $\epsilon$ , and  $\Gamma$  at 2.6 Mev has been tabulated for rough comparison

with the other resonances. The actual thick target yield at any energy from this reaction can be obtained from Figure 8.

A second feature of the cross section as presented in Figure 15 is the anomaly at about 700 kev. It is also present when the cross section is obtained from the thick gas target although it is not as striking, being smeared out over a larger energy range. The fit to the dispersion formula has been so satisfactory at energies above 900 kev that this can most reasonably be explained by assuming a small resonance in this region. A resonance at 700 kev with  $\sigma_R = 1 \times 10^{-30} \text{ cm}^2$  and  $\Gamma = 100 \text{ kev}$  will fit the data. A value of  $Y_{\text{max}}(\infty)$  can then be calculated.

A complete description of the experimental cross section from .250 to 2.6 Mev is therefore obtained by giving the values of  $E_R$ ,  $\Gamma$ ,  $Y_{\text{max}}(\infty)$ , and  $\sigma_R$  for various resonances. This data is tabulated below.

TABLE 2

$E_R$ (Mev)	$\Gamma$ (kev)	$Y_{\text{max}}(\infty)$ ( $\beta^+$ /proton)	$\sigma_R$ ( $\text{cm}^2$ )
.277	< 2	$.35 \pm .03 \times 10^{-10}$	$> 1.5 \times 10^{-28}$
.70 $\pm$ .03	100 $\pm$ 30	.2 $\pm$ .07	0.01
1.065 $\pm$ .002	4.8 $\pm$ 1	5.5 $\pm$ .1	3.7
1.55 $\pm$ .02	50 $\pm$ 20	1.2 $\pm$ .2	0.06
1.748 $\pm$ .005	11 $\pm$ 3	1.5 $\pm$ .3	0.3
1.815 $\pm$ .004	7 $\pm$ 1.5	3.7 $\pm$ .3	1.1
2.356 $\pm$ .008	14 $\pm$ 4	15 $\pm$ 2	2.1
2.489 $\pm$ .007	11 $\pm$ 3	21 $\pm$ 1	3.5
2.60* $\pm$ .05	1270 $\pm$ 50	300 $\pm$ 50	0.5

\* Data for this resonance has been corrected for penetration effects.

Before proceeding with the discussion of these quantities, it will be well to consider the probable errors which have been ascribed to them. The resonance energy is known with the greatest percentage precision. Its accuracy depends on the magnetometer constant and upon the precision with which the resonance energy can be determined from the excitation curves. The value of  $k$  can be determined to within 0.03% from the aluminum curves. Using the same value of  $k$ , as was done in all cases except with the  $\text{Be}_3\text{N}_2$  curve introduces a 0.1% error. The accuracy of determining the magnetometer millivolts for resonance varies for the different resonances. Where the value can be determined from the  $\text{Be}_3\text{N}_2$  curve, the value obtained has a probable error of about 0.1%. The value at the 1.55 resonance, being determined from the gas target, has a probable error of about 20 kev; the values at the broad resonances at .70 and 2.6 Mev about 30 and 50 kev respectively. The layers of carbon on the target introduce an additional source of error. This was appreciable only in the case of the values determined from the  $\text{Be}_3\text{N}_2$ . The frequent changing of targets and the use of a liquid air trap are believed to have limited this error to 1 kev or less. This way the probable errors on  $E_R$  given above were determined.

In discussing the quantities involving yield, it is necessary to know the probable errors of  $c$ ,  $n$ ,  $\lambda$ , and  $f$ . The statistical error in the counting rate is given wherever possible on all of the curves. Where none is indicated, it is less than or equal to the size of the points. The integrator is believed to introduce a negligible error. As indicated above,  $\lambda$  is known to 2%. Thus it should be possible to obtain moderately accurate relative values for the various parameters at the different resonances. Actually

the largest probable error comes from the uncertainty arising in drawing the appropriate curve through the experimental points. For example, with the  $\text{Be}_3\text{N}_2$  curves, the statistical uncertainty was usually only about 1%; but with a thick target step about 20% of the total yield, this introduces an appreciable uncertainty. The relative errors vary from resonance to resonance, but are usually about 2 - 10%. Estimates are given above.

There are additional uncertainties in the absolute value of these quantities. The capacitance is known to  $\frac{1}{2}\%$ . The corrections for "vacuum activity", leakage of nitrogen from the chamber, and absorption of positrons in the copper foil are believed to be well known, introducing an error of a few percent at most. The largest uncertainty is in the counting efficiency,  $f$ . The quantities entering Equation 4 for its evaluation, the counting efficiency over the face of the counter and the geometrical distances, are known with sufficient precision. However the evaluation of  $f$  involves four repeated integrations. By carrying out calculations with similar but integrable functions, it is estimated that each of the integrations is accurate to 2% or better. Thus the total error should be less than 8%. One can therefore place an error on the over-all absolute normalization of 10%.

The probable errors on the widths come from the inaccuracies involved in fitting a curve to the points. The curves from the thin layer gave a very low yield, so that the statistical errors are moderately large as indicated. Estimates are given for the errors.

There are several possible corrections which have not been made. The reasons for neglecting them should be mentioned. Since



the counting rates were sufficiently small, no appreciable error was made in neglecting the dead time of the counter.

It has been assumed that the distribution of  $O^{15}$  is uniform throughout the gas target; this is certainly not true initially since the gas is formed in the center where the beam passes through. The diffusion problem for such a case can be solved in a more or less rigorous manner; however an order of magnitude calculation can be used to demonstrate that the time for the concentration to become uniform is quite small. The order of magnitude of the time is given by Einstein's equation as

$$t = \frac{3\pi \eta a x^2 n}{RT} \quad (12)$$

where  $\eta = 1.75 \times 10^{-4}$  poise is the coefficient of viscosity,  $a = 1.9 \times 10^{-8}$  cm is the molecular radius,  $x = 1$  cm is the radius of the chamber,  $n = 2 \times 10^{18}$  molecules  $\text{cm}^{-3}$  (for a typical experiment) is the molecular density,  $R = 8.3 \times 10^7$  erg  $\text{deg}^{-1}$  mole $^{-1}$  is the gas constant, and  $T = 300^\circ$  is the absolute temperature. Carrying out the arithmetic gives  $t = 2.5 \times 10^{-3}$  seconds, so that the assumption of uniform density introduces a negligible error.

Various other quantities can now be calculated which are of considerable interest. The quantity  $\omega\gamma$  which is defined as  $\omega \Gamma_\gamma \Gamma_p (\Gamma_\gamma + \Gamma_p)^{-1}$  can be determined for each of the resonances.  $\Gamma_\gamma$  can be calculated for the various types of gamma radiation which are possible and is always of the order of several electron volts or less. The observed widths,  $\Gamma = \Gamma_p + \Gamma_\gamma$ , must therefore be equal to  $\Gamma_p$ , so that  $\omega\gamma = \omega \Gamma_\gamma$ .

Another quantity of theoretical interest in discussing the

results is the width for proton emission at 1 Mev without barrier,  $G$ , which is related to the observed width by the previously mentioned equation  $\Gamma = E^{\frac{1}{2}}PG$ . The values of  $G$  obtained will depend on the  $l$  value of the protons initiating the reaction, which in general is not known. It is therefore necessary to give values corresponding to  $s$ ,  $p$ , and  $d$  waves.

In this way values have been obtained for each of the quantities entering the Breit-Wigner formula for the cross section, and it is possible to calculate a value of the cross section at any energy due to each of the resonances. The total cross section will not necessarily be the sum of these values since it is the amplitudes and not the absolute values of the waves which are additive. Nevertheless it is possible to obtain some idea of the contribution to the total cross section that each of the resonances makes at a particular energy.

It is of considerable interest to know the value of the cross section at very low energies, because of the importance of the reaction as a possible source of stellar energy. For this reason the value of the cross section at 128 kev and 28 kev for each of the resonances has been calculated. The value at 128 kev is given because the total cross section has been measured at this energy.<sup>(4)</sup> The value at 28 kev is given because this is the approximate energy of interest in stellar calculations. In each case the resonances have been assumed to be due to  $s$  wave protons, since this gives an upper limit on the value obtained. As we shall see the resonances that make an important contribution do seem to be caused by  $s$  wave protons.

In this way the quantities appearing in Table 3 have been

calculated. They are of value in describing the reaction, but are calculated from the experimental data rather than being directly observable.

TABLE 3

$E_R$ (Mev)	$\omega/\gamma$ (ev)	G(s) (kev)	G(p) (kev)	G(d) (kev)	$\sigma$ (128) ( $10^{-11}$ barns)	$\sigma$ (28) ( $10^{-21}$ barns)
.277	0.02	<3,000	<20,000	<70,000	< 2.5	< 1.5
.70	0.02	1,700	8,000	15,000	1.1	1.5
1.065	0.63	24	80	960	0.02	0.03
1.55	0.16	110	250	2,000	0.01	0.02
1.748	0.31	20	44	280	0.0015	0.003
1.815	0.52	12	27	170	0.002	0.004
2.356	2.4	17	28	140	0.007	0.015
2.489	3.3	12	20	85	0.007	0.015
2.60	46	1,250	-	-	8.7	15.0

The energy of each level above the ground state of  $O^{15}$  can also be determined and an energy level diagram constructed. The energy of each level is given by

$$E = Q + \frac{M(N^{14})}{M(O^{15})} E_R \quad (13)$$

where  $Q = M(N^{14}) + M(H^1) - M(O^{15}) = 7.29 \text{ Mev}$  (14)

Values are tabulated below:

TABLE 4

$E_R$	.28	.70	1.06	1.55	1.75	1.82	2.36	2.49	2.60
E	7.55	7.94	8.28	8.74	8.92	8.98	9.46	9.61	9.72

The sum of all the cross sections at 128 kev is  $1.24 \times 10^{-10}$  barns, which is to be compared with the measured value of  $7 \times 10^{-10}$  barns. If these values are both believed to be correct, this is evidence for an additional resonance at low energies. It is quite possible that there exists a level which would make an appreciable contribution at 128 kev but which would not contribute to the cross section at stellar energies. Should this be the case, the correct value of the cross section at 28 kev would be  $9 \times 10^{-20}$  barns, instead of  $6 \times 10^{-19}$  as inferred from the low energy work. Such a low cross section would make it exceedingly difficult to explain the observed energy release at stellar temperatures with the carbon-nitrogen cycle. Since the levels of  $O^{15}$  are quite closely spaced at this excitation energy, the probability that there is a resonance in the stellar region is not negligible; such a resonance would make any extrapolation of values from energies where the cross section is measurable incorrect.

The widths for  $\gamma$ -ray emission for each of the levels have been determined. If the energy of the  $\gamma$ -ray were known, this would permit the evaluation of the associated oscillator strength. The determination of the  $\gamma$ -ray spectrum was not attempted. The major problems which make such a determination a very difficult experimental problem are the low cross section, making the accumulation of sufficient points a lengthy and inaccurate process, and the presence of  $\gamma$ -rays from the  $N^{15}(p, \alpha \gamma)C^{12}$  reaction which gives a larger thick target yield from a non-enriched target than the desired reaction. There are also very large competing  $\gamma$ -ray yields from any of the targets which were found to be satisfactory: from the  $Be(p, \gamma)$  reaction in the case of the  $Be_3N_2$

target and from the  $\text{Al}(p, \gamma)$  reaction in the case of the gas target.

To make more precise the nature of the difficulties in making such a measurement, consider the expected results from an experiment, assuming there is no competing radiation except from the  $\text{N}^{15}$ . The cross section for the  $\text{N}^{15}(p, \alpha\gamma)\text{C}^{12}$  reaction at 1.065 Mev, the most favorable energy for the experiment, is relatively constant and equal to  $1.2 \times 10^{-26} \text{ cm}^2$ . (15) Multiplying this by the abundance of  $\text{N}^{15}$  gives a relative cross section of  $4.3 \times 10^{-29}$ . This is to be compared with the resonant cross section for the  $\text{N}^{14}$  reaction of  $3.7 \times 10^{-28}$  and a non-resonant cross section of  $4 \times 10^{-30}$ . The most favorable target thickness would be equal to the resonance width, 5 kev. If such a target could be made from KCN,  $\text{KNO}_3$ , TiN, or  $\text{CaCN}_2$  with about 30% nitrogen, the yield from the desired resonance would be one half the thick target step, or  $9 \times 10^{-11}$  quanta per proton. The yield from the  $\text{N}^{15}$  reaction would be  $1.3 \times 10^{-11}$ . With the maximum beam strength and solid angle used during this experiment and assuming the transition is to the ground state giving a gamma ray of 8 Mev energy which can be counted with 6% efficiency, a counting rate of about 350 counts per minute would be expected. Even under these most favorable of assumptions, the accumulation of sufficient data to determine the energy spectrum of the gamma ray by any of the usual techniques would be exceedingly difficult.

Gamma ray widths can be described theoretically in different ways. The fundamental formula for electromagnetic radiation is

$$\Gamma_{\gamma} = \frac{32 \pi^3}{3} \frac{v^3}{c^3} D_{mn}^2 \quad (15)$$

where  $D_{mn}$  is the matrix element between the initial and final states.

For electric multipole radiation Bethe<sup>(16)</sup> expresses  $D_{mn}$  in terms of the oscillator strength by

$$f_{mn} = 4\pi\nu \hbar^{-1} (D_{mn}/e)^2 \quad (16)$$

Fowler, Lauritsen, and Lauritsen<sup>(10)</sup> express  $D_{mn}$  in terms of the ratio of  $r$  to  $r_0$ , where  $er^l$  is the matrix element for the electric  $2^l$  pole radiation and  $r_0$  is the classical electron radius. Bethe's definition has the advantage in the case of dipole radiation that an expression for  $\sum |f_{no}|$ , the sum of the oscillator strengths for all levels to the ground state, is calculable and gives an upper limit on the value of  $\Gamma_\gamma$ .

For the case of electric quadripole radiation, the sum rule applies to  $f_{mn}(\hbar\nu)^{-1}$ , so this would seem to be the more appropriate quantity to discuss. For magnetic dipole radiation,  $\mu/\mu_N$  is evaluated. The quantities tabulated below for each resonance are therefore  $f_{no}$ ,  $r/r_0$  for electric dipole,  $r/r_0$  for electric quadripole, and  $\mu/\mu_N$ . They are calculated with the statistical weight factor,  $\omega$ , set equal to 1. If detailed use is to be made of them, appropriate values of  $\omega$  can be used. The formulas used for calculation are

$$\begin{aligned} f_{no} &= 0.191 \Gamma_\gamma (\hbar\nu)^{-2} \\ r/r_0 &= 0.7 \Gamma_\gamma^{\frac{1}{2}} (\hbar\nu)^{-3/2} \quad \text{electric dipole} \\ r/r_0 &= 7 \Gamma_\gamma^{\frac{1}{4}} (\hbar\nu)^{-5/4} \quad \text{electric quadripole} \\ \mu/\mu_N &= 19 \Gamma_\gamma^{\frac{1}{2}} (\hbar\nu)^{-3/2} \end{aligned} \quad (17)$$

These values will be increased if  $\omega < 1$ , as is probably true in most cases; or if the transition is to some level other than the

ground state.

TABLE 5

$E_R$ (Mev)	$f_{no}$	$r/r_0$ el. dipole	$r/r_0$ el. qdpole	$\mu/\mu_N$ mag. dipole
.277	.00007	.005	.21	.13
.70	.00006	.0045	.20	.12
1.065	.0018	.024	.45	.65
1.55	.0004	.011	.30	.30
1.748	.0005	.012	.31	.33
1.815	.0012	.019	.39	.52
2.356	.005	.037	.53	1.0
2.489	.007	.043	.56	1.2
2.60	.09	.16	1.1	4.3

Unfortunately the rigorous sum rules do not give limits very useful here. The maximum value of  $f_{no}$  for dipole radiation is somewhat larger than  $AZ/N$ ,<sup>(17)</sup> a value not approached here. For electric quadripole radiation the maximum value is

$$\left(\frac{f_{no}}{h\nu}\right)_{\max} = \frac{4}{9} \alpha^2 \frac{T_{00}}{(mc^2)^2} \quad (18)$$

where  $\alpha$  is the fine structure constant and  $T_{00}$  is the kinetic energy of all the protons in the ground state.<sup>(17)</sup> Substituting this in Equations 15 and 16 gives the maximum value of  $\Gamma_\gamma$  to be 22 ev. It thus seems possible to rule out electric quadripole radiation in one case. The value of  $\mu/\mu_N$  for this resonance seems quite large, but one would not expect a sum rule for magnetic dipole radiation to rule out values less than  $Z\mu_N$ .

From the values of  $G$  given in Table 3, it is possible to make certain statements concerning the  $l$  values of the protons. Values of  $G$  corresponding to a half life less than the transit time of a proton across the nuclear diameter are not possible. This gives an upper limit to  $G$  of about 2 Mev. It does not seem possible to give a lower limit, but a very rough value may be tentatively taken as 100 kev. If  $G$  is to be confined to these limits, the  $l$  values of the protons for the various resonances can be determined as follows:

TABLE 6

E	.277	.700	1.065	1.55	1.748	1.815	2.356	2.489	2.60
R									
l	s	s	p-d	s-d	>d	>d	>d	>d	s

The s wave assignment for the .277 Mev resonance assumes that the observed width is greater than 0.1 kev. Although this seems reasonable from Tangen's published curve, it must be remembered that the only value he gives is that the width is less than 2 kev.

The ground state of  $N^{14}$  has a spin 1, but the parity is not definitely known. It has always been assumed to be even, but Wigner and Feingold<sup>(18)</sup> have recently found that they are able to fit the half life of  $C^{14}$  more consistently into a scheme of beta decay if the parity is taken as odd. The ground state of  $N^{14}$  can then be taken for future discussion as spin 1 and parity  $\pm$ . The compound nucleus formed then will have angular momentum and parity as follows:



TABLE 7

l value of proton	s	p	d
J value of $O^{15*}$	1/2;3/2	1/2;3/2;5/2	1/2;3/2;5/2;7/2
Parity of $O^{15*}$	$\pm$	$\bar{+}$	$\pm$

The ground state of  $O^{15}$ , a mirror nucleus with respect to  $N^{15}$ , may be taken as having a spin  $\frac{1}{2}$  and odd parity.

The level where the assignment of both the l value of the protons and the type of gamma radiation is most definite is the 2.60 Mev level. S wave protons form a level with angular momentum 1/2 or 3/2, which then decays by electric dipole radiation to a level of spin 1/2, 3/2, or 5/2. If this is the ground state with odd parity, the parity of the compound nucleus and hence of the ground state of  $N^{14}$  must be taken as even. The higher energy levels can easily and non-uniquely be fitted into this scheme.

A difficulty is presented by the resonances at .277 and .700 Mev which have been assigned to s wave protons. With the above assignment of parity to  $N^{14}$ , these would be 1/2 or 3/2 levels with even parity; however, the corresponding values of the oscillator strength for electric dipole radiation are only 7 and  $6 \times 10^{-5}$  respectively. Although such values are presumably possible, they do seem to be unusually small for the transition to the ground state which would be allowed.

If the ground state of  $N^{14}$  is taken as spin 1 and odd parity, the radiation from the 2.6 Mev resonance must be magnetic dipole if it is to the ground state; or if it is electric dipole as the intensity indicates, the transition must be to a level in  $O^{15}$  near

the ground state but with even parity. Although no such level is known and indeed there are no low lying levels in the mirror nucleus  $N^{15}$ , where the spectrum has been more completely explored, (19) its existence is certainly possible. If this level is given a spin of  $5/2$  and the two levels at .377 and .700 Mev are given a spin of  $1/2$ , electric dipole transitions between them will be forbidden. The 2.6 Mev level will then be assigned a spin of  $3/2$ . Once again, the higher energy levels can be filled into this scheme.

There is certainly not enough evidence from intensity relations alone to make conclusive level assignments. The above arguments are presented as merely a first step towards some future definite assignment of the level structure of  $O^{15}$ . Useful information to help in assigning the  $l$  values of the protons might be obtained by studying the scattered protons. Other information which would be of value would be the energy spectrum and the angular distribution of the gamma radiation. The experimental difficulties of working directly with the  $\gamma$ -rays have been previously discussed.

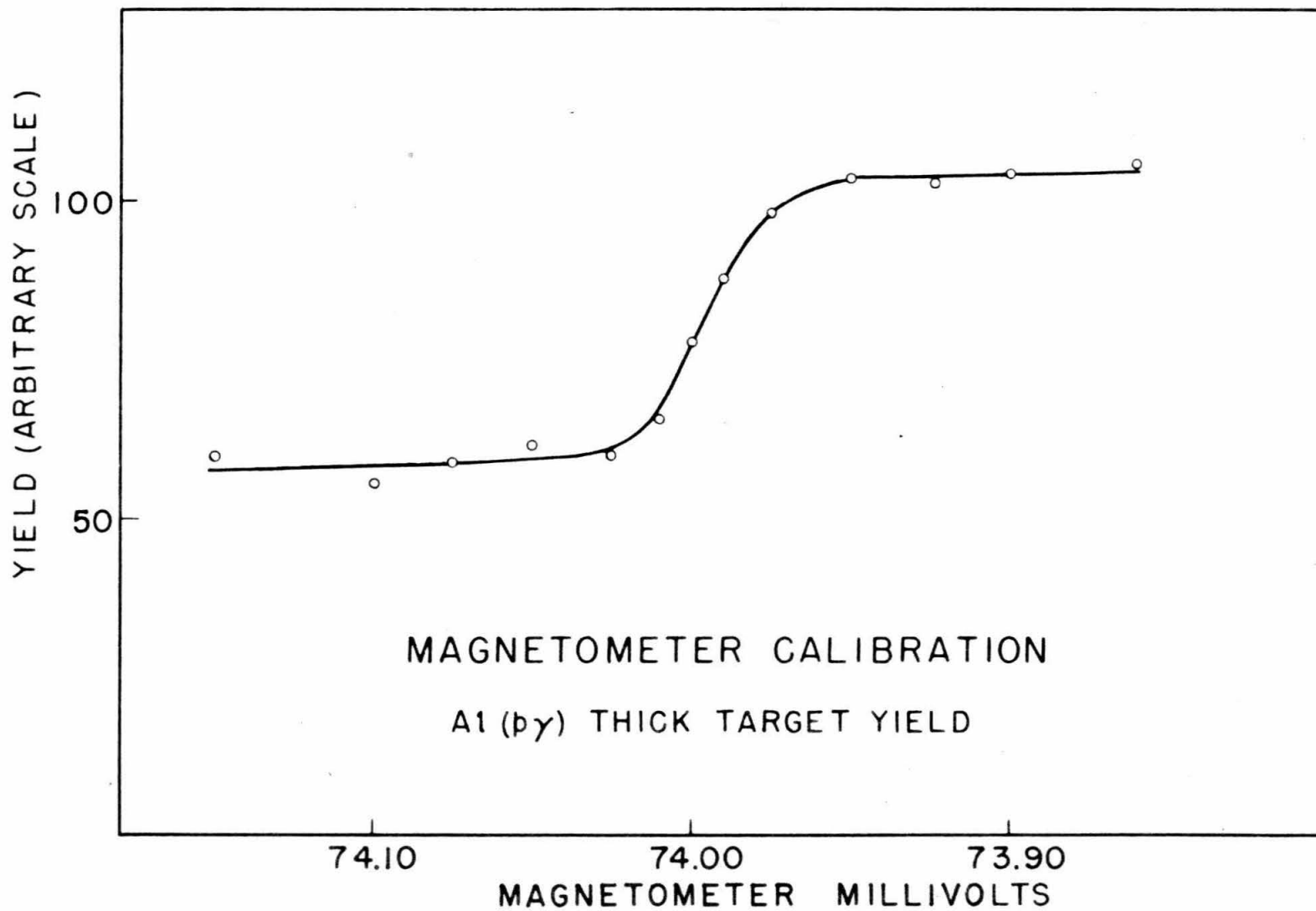
It is also possible to make a few remarks concerning the general excitation curve and the level characteristics. The average level spacing is about 250 kev. The sharp resonances near 1.8 and 2.4 Mev appear to be doublets, although the possibility exists that they are merely accidentally close. Such doublet structure levels split by about 20 to 50 kev and separated by about 1 Mev, is known in both  $N^{15}$  and  $O^{16}$ . A possible explanation of these, given by Inglis, (20) is that the coupling between a nucleon excited into a higher  $s$  shell and the remaining  $p$ -shell structure gives adjacent states differing by one in the value of  $J$ . Although

the data here is consistent with such a picture, it would be very remarkable if a two body interaction model is sufficient. Certainly more definite values for the angular momentum and parity of the various states must be obtained before it is possible to draw any conclusions.

As predicted by the dispersion formula, the thick target yields of the various resonances show no marked dependence on proton energy. The values of  $G$ , however, do not seem to be quite so consistent with what is expected, seeming to decrease at higher proton energies. The absence of broad levels at higher energies can be explained by the experimental difficulties of observing them. However, as in the cases of the  $C^{12}(p, \gamma)$  and  $C^{13}(p, \gamma)$  reactions, there seems to be no immediate explanation for the fact that the levels excited by low proton energy have large values of  $G$ . Once again there is not enough information to indicate that this is more than accidental.

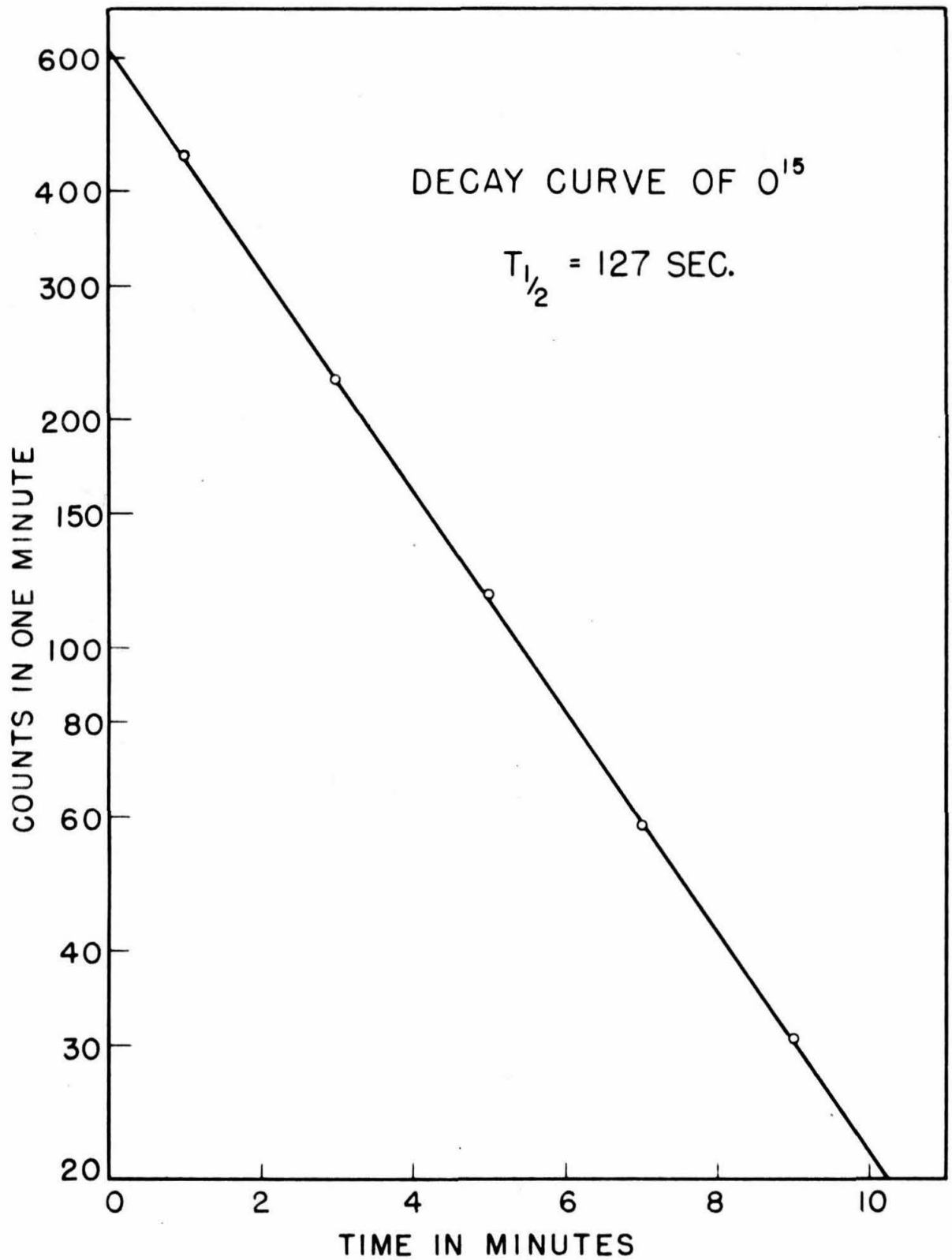
REFERENCES

1. DuBridge, Barnes, Back, and Strain, Phys. Rev. 53, 447 (1938).
2. Curran and Strothers, Nature 145, 224 (1940).
3. Tangen, Kgl. Nord. Vid. Selsk. Skr. No. 1 (1946).
4. Woodbury, Hall, and Fowler, Phys. Rev. 75, 1462(A) (1949).
5. For Example; Lauritsen, Lauritsen, and Fowler, Phys. Rev. 59,  
241 (1941).
6. Duncan, Phys. Rev. 76, 587(A) (1949).
7. Lauritsen and Lauritsen, Rev. Sci. Inst. 19, 916 (1948).
8. Herb, Snowden, and Sala, Phys. Rev. 75, 246 (1949).
9. Livingston and Bethe, Rev. Mod. Phys. 9, 245 (1937).
10. Fowler, Lauritsen, and Lauritsen, Rev. Mod. Phys. 20, 236 (1948).
11. Bernet, Herb, and Parkinson, Phys. Rev. 54, 398 (1938).
12. Bethe, The Properties of Atomic Nuclei, June 1 (1949), B.N.L.-  
T - 7.
13. Madson and Venkateswarla, Phys. Rev. 74, 648 (1948).
14. Christy and Latter, Rev. Mod. Phys. 20, 185 (1948).
15. Schardt, Priv. Comm.
16. Bethe, Rev. Mod. Phys. 9, 69 (1937).
17. Levinger and Bethe, Phys. Rev. 78, 115 (1950).
18. Feingold and Wigner, Priv. Comm. to Professor R. Christy.
19. Lauritsen, Hornyak, Morrison, and Fowler, Rev. Mod. Phys.  
Oct. (1950).
20. Inglis, Phys. Rev. 78, 616 (1950).



- 38 -  
FIGURE 1

-39-  
FIGURE 2



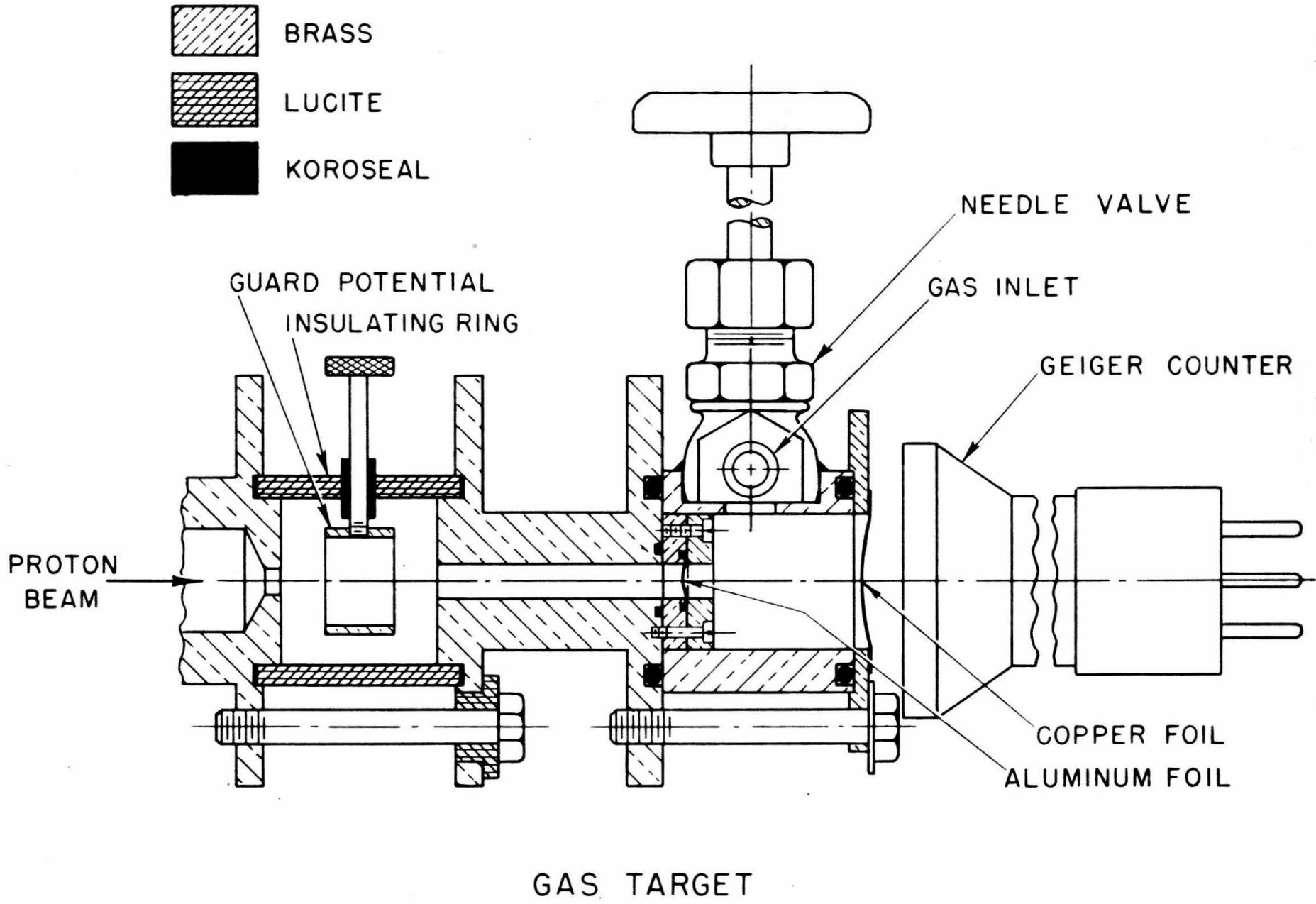


FIGURE 3  
-40-

# COUNTING EFFICIENCY OVER THE FACE OF A BELL JAR COUNTER

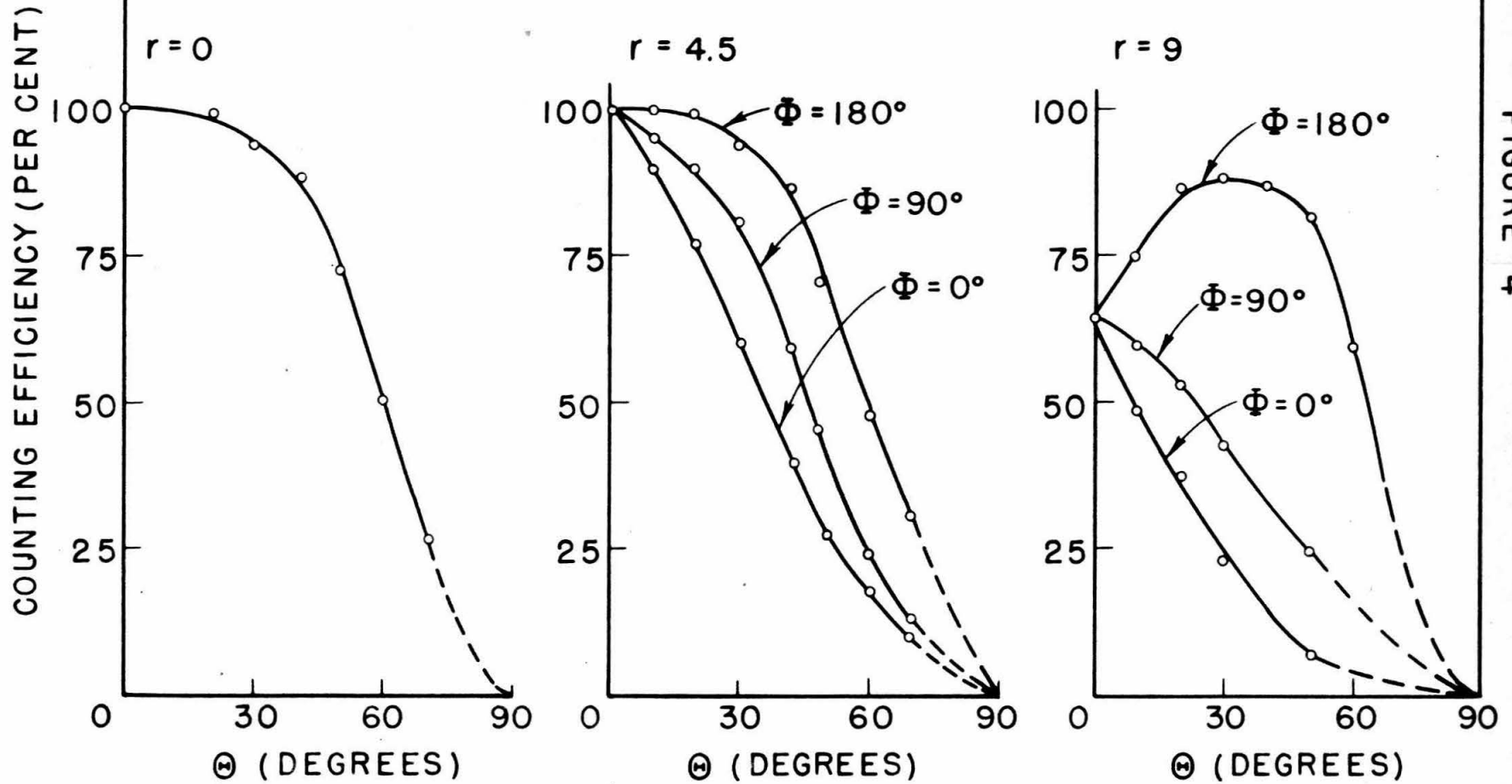


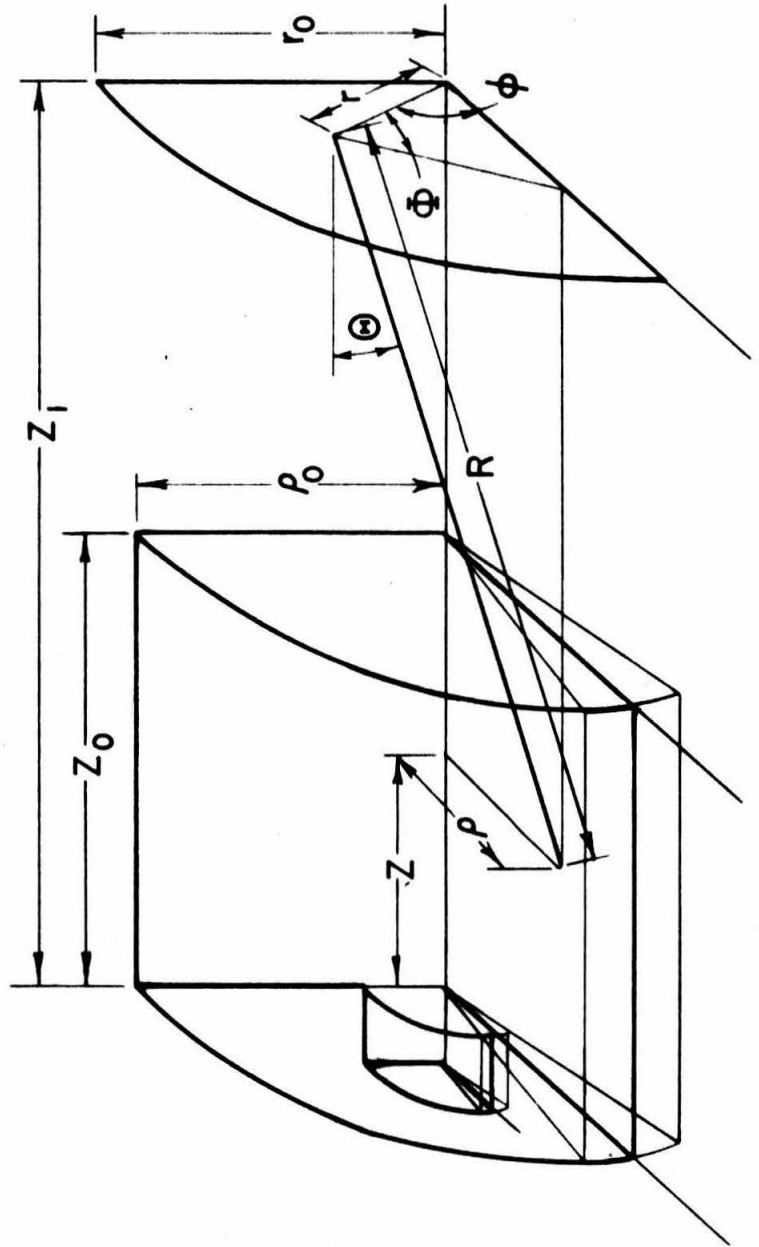
FIGURE 4

-4/-



FIGURE 5

ILLUSTRATION OF COUNTING EFFICIENCY EVALUATION



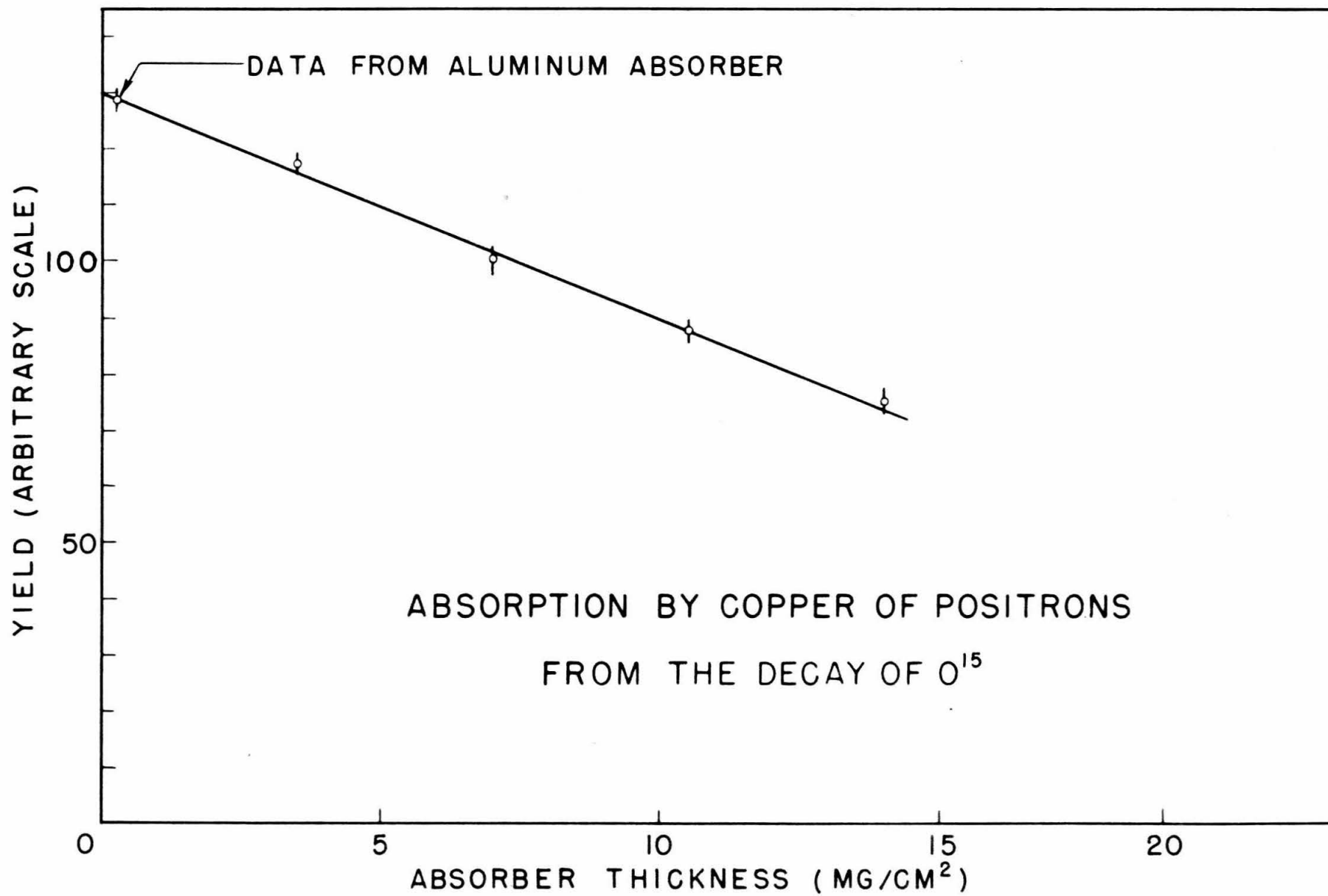
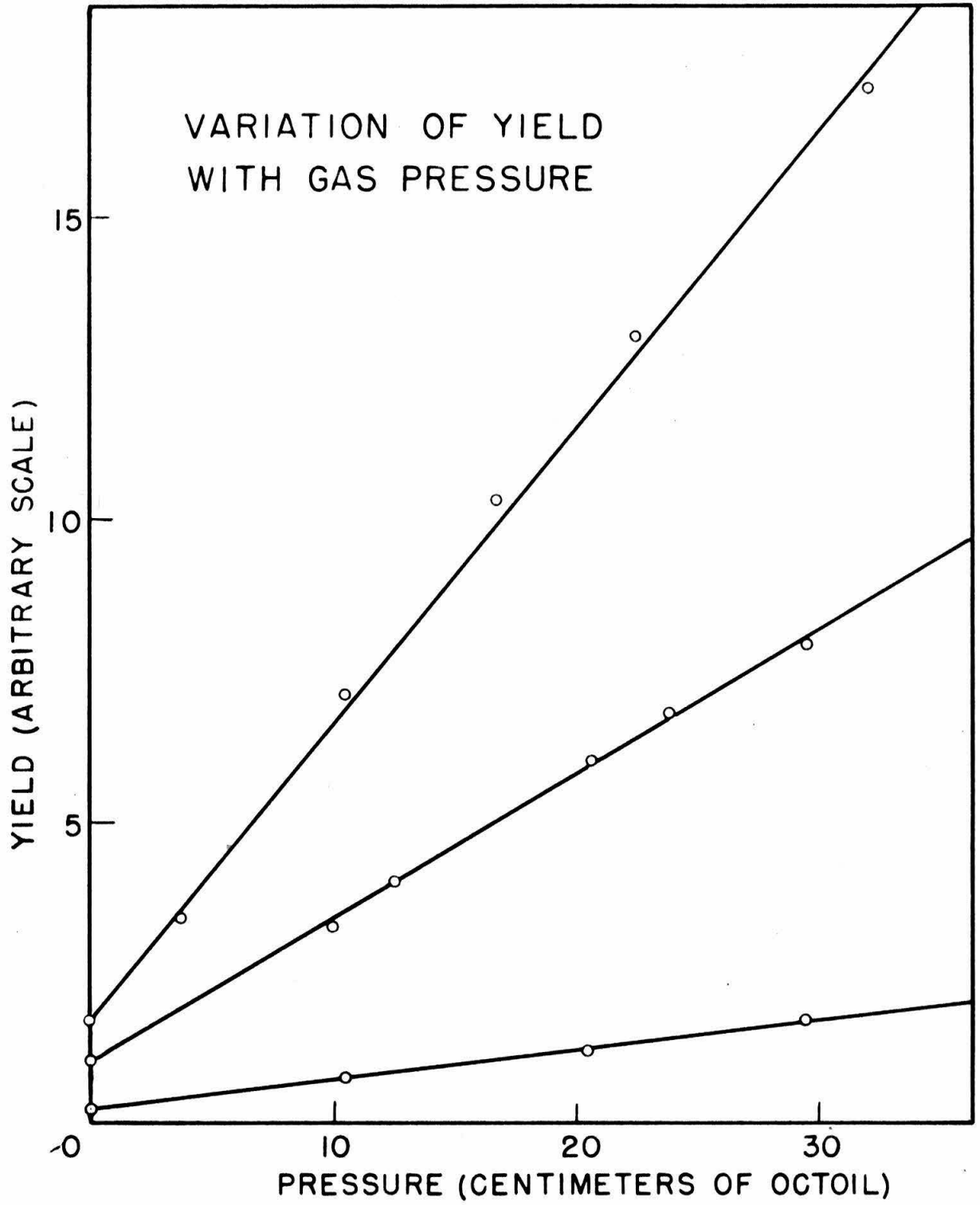
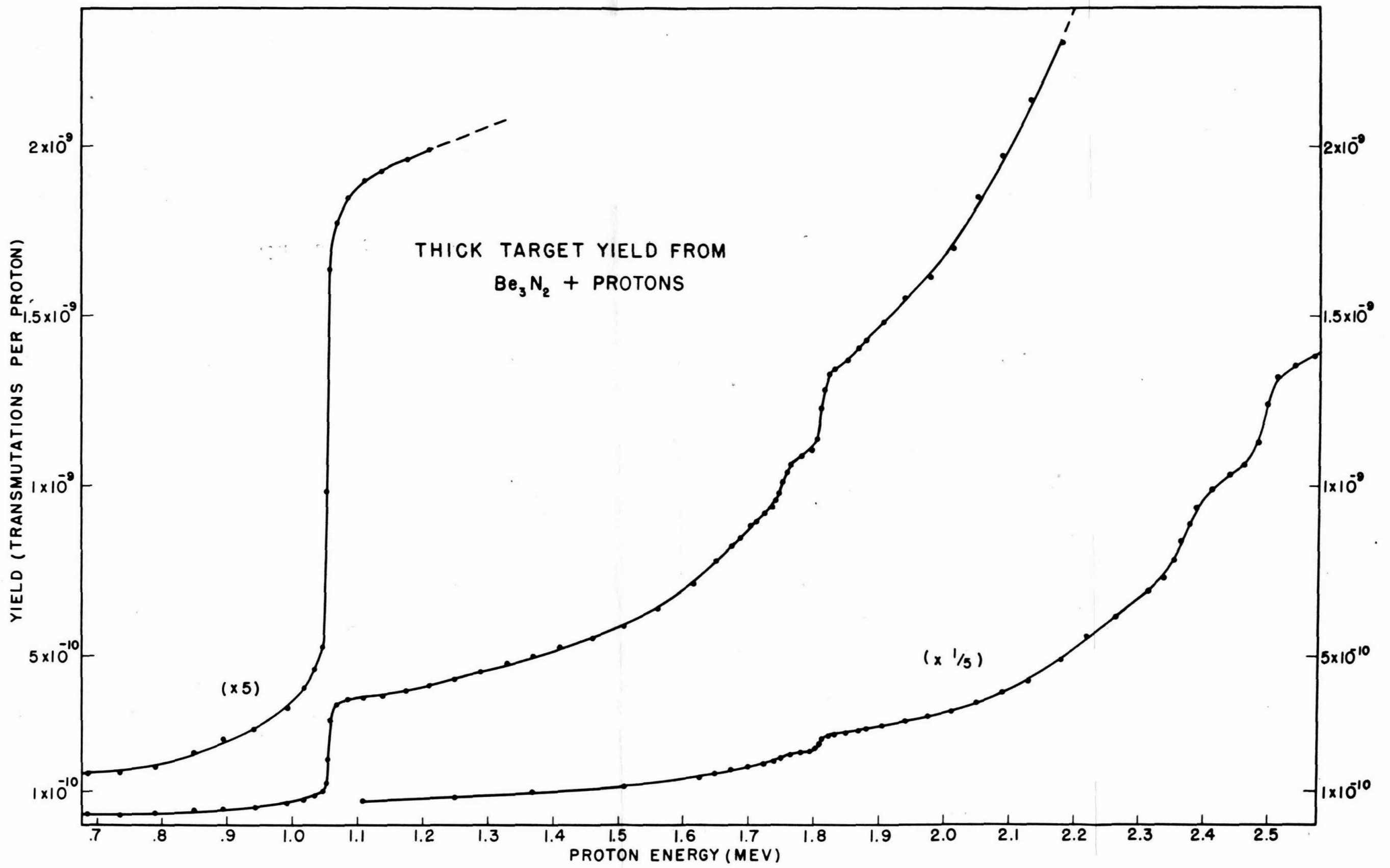
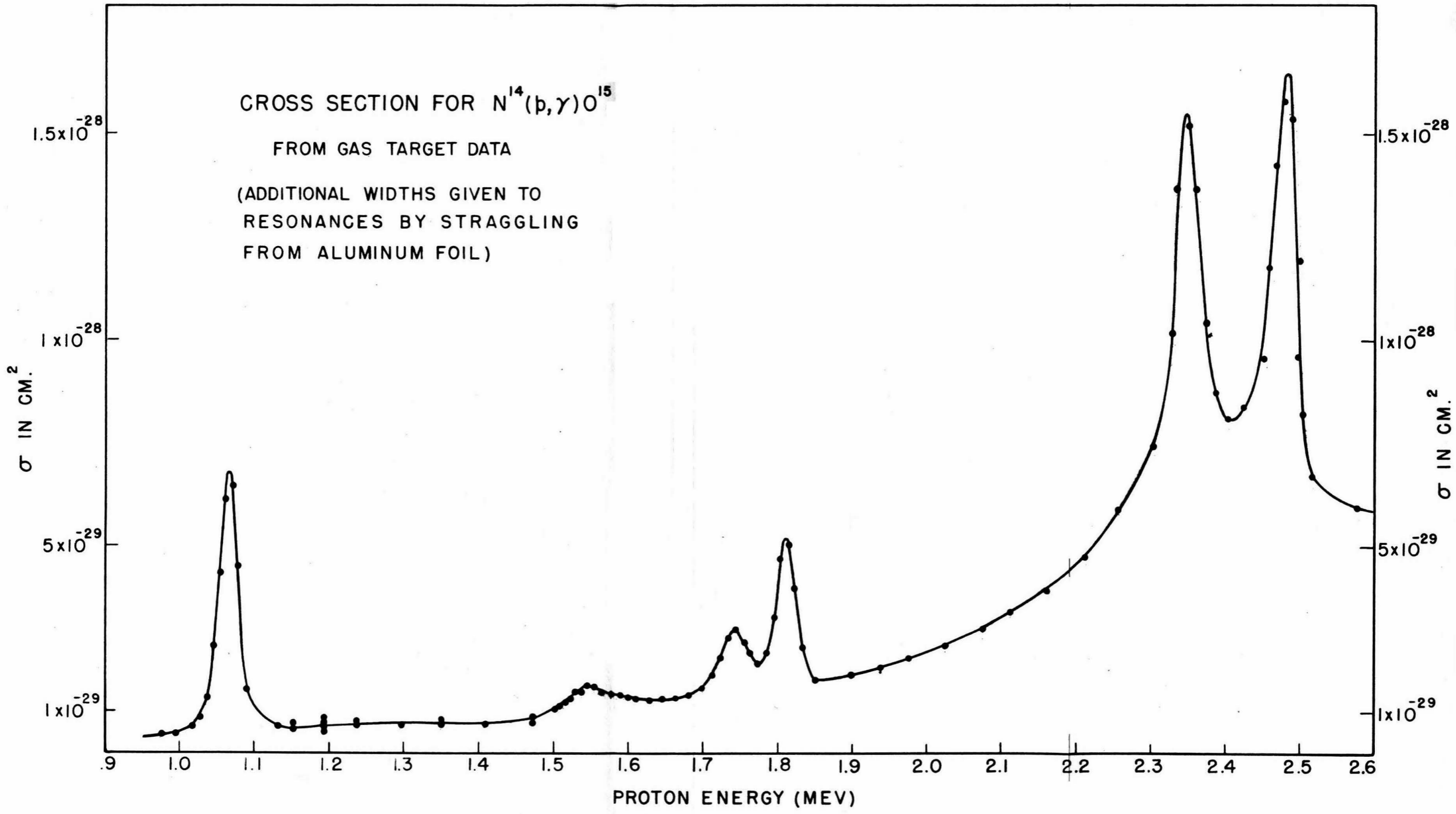


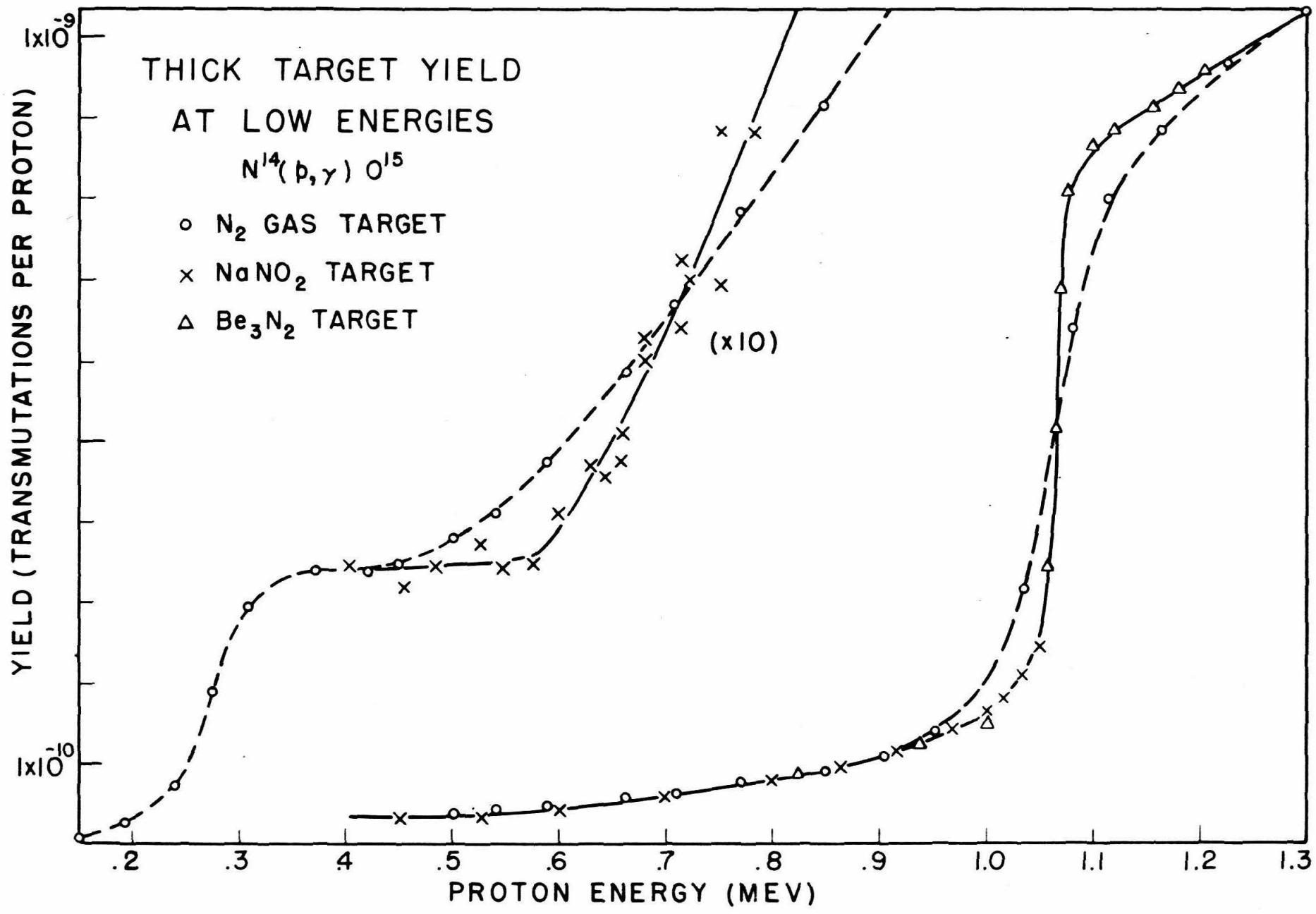
FIGURE 6

FIGURE 7









-47-  
FIGURE 10

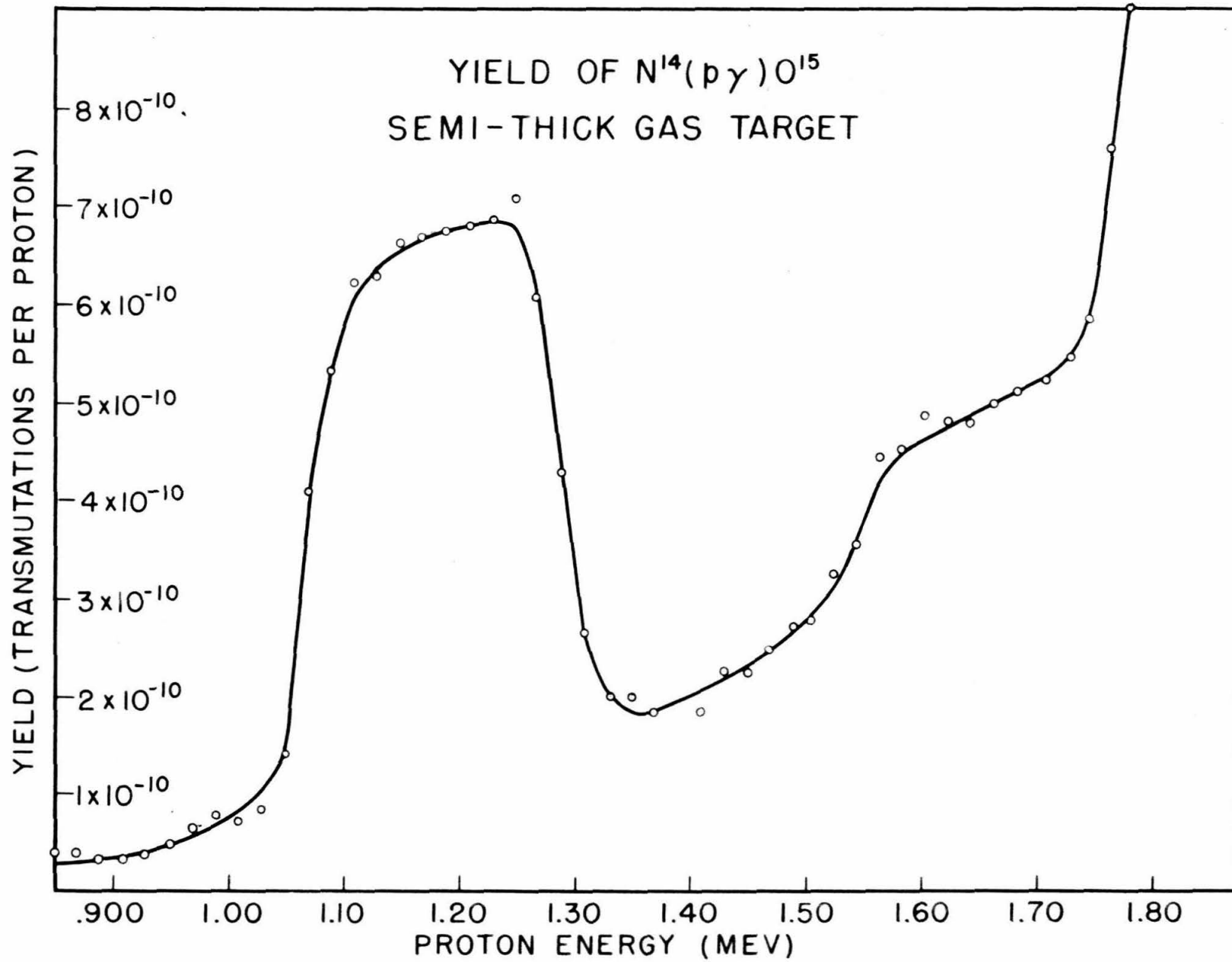
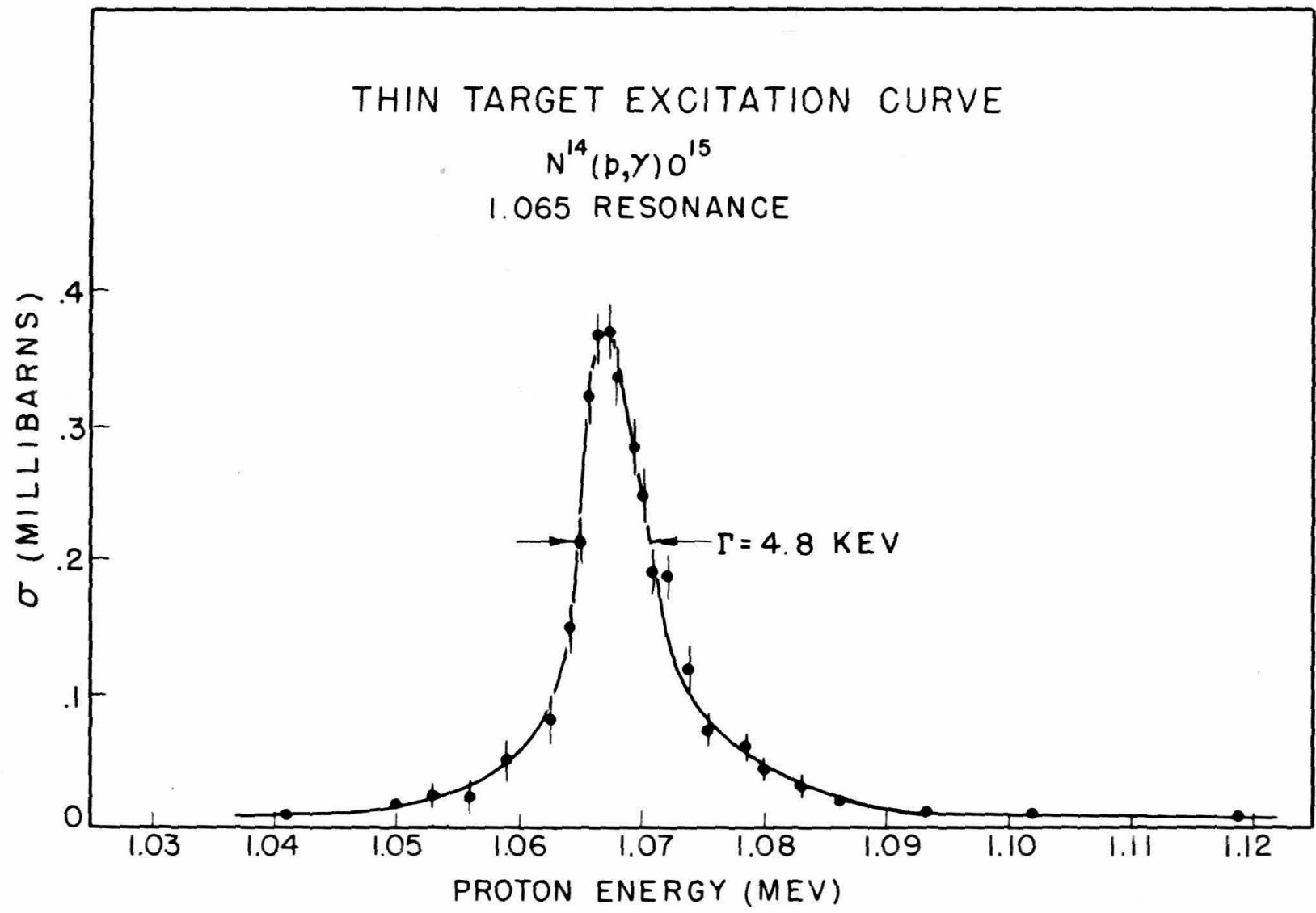


FIGURE 11

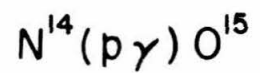
-49-

FIGURE 12





THIN TARGET EXCITATION CURVE



1.815 RESONANCE

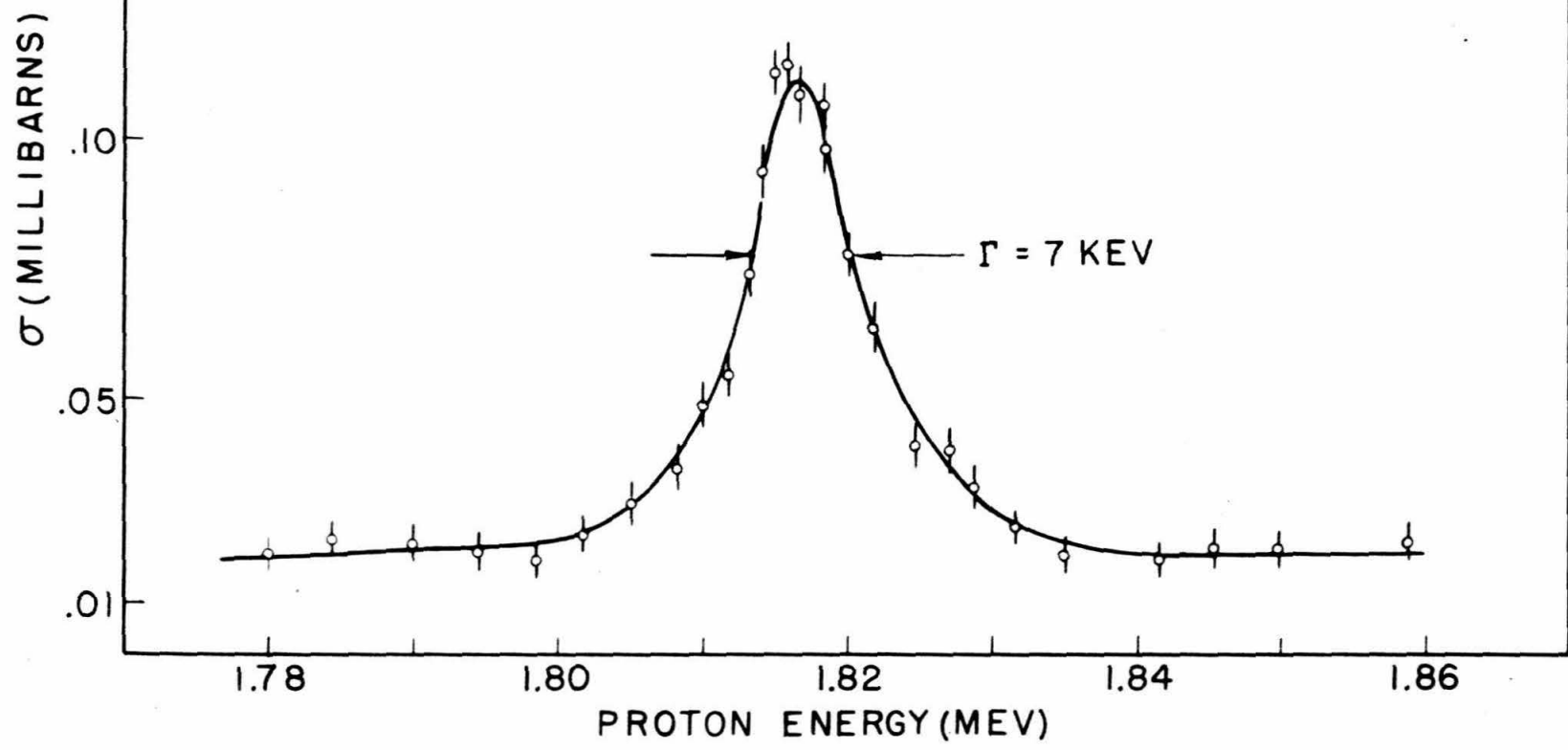


FIGURE 13

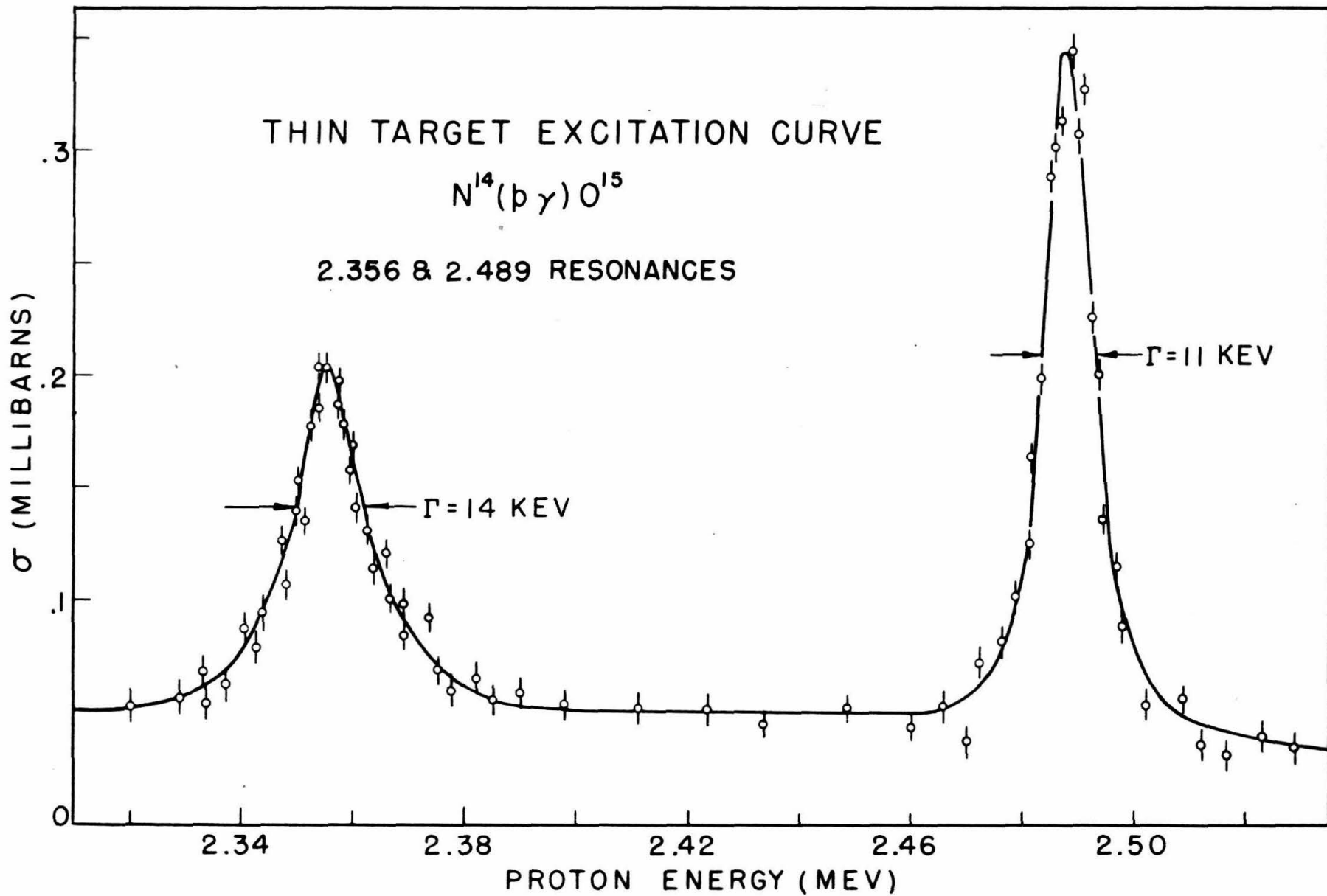
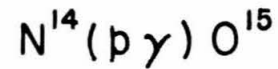


FIGURE 14

"NON-RESONANT" CROSS SECTION



- THIN GAS TARGET
- △ THICK  $Be_3N_2$  TARGET SLOPE
- × THICK  $NaNO_2$  TARGET SLOPE

.05

σ (MILLIBARNS)

(x10)

THEORETICAL CURVE

$G = 1.27$  MEV

$E_R = 2.6$  MEV

$\omega\Gamma_\gamma = 45$  EV

S WAVE PROTONS

.01

.5

1.0

1.5

2.0

2.5

PROTON ENERGY (MEV)

FIGURE 15  
-52-